



Sequential large momentum transfer exploiting rectangular Raman pulsesB. Dubetsky ^{*}*1849 South Ocean Drive, Hallandale, Florida 33009, USA* (Received 27 May 2023; revised 25 September 2023; accepted 3 November 2023; published 8 December 2023)

It is proposed to use rectangular Raman pulses for the technique of sequential large momentum transfer. It is shown that the small parameters that make it possible to use this technology for precision atom interferometry can be 40–200 times smaller than in the case of the Bragg regime. It is predicted that in the case of a nonequidistant timing of auxiliary pulses, one can observe oscillations in time of the interference picture with a period inversely proportional to the recoil frequency. Such an observation would be confirmation that Mach-Zehnder atom interference is a phenomenon caused by the quantization of the atomic center-of-mass motion. This effect is calculated for any shape of pulses. One can observe it in the Bragg regime as well. It is proposed to use noncontinuous composite Raman pulses as auxiliary beam splitters so that the effective Rabi frequency remains unchanged for the entire process. The gravity phase of an atomic interferometer is calculated for any shape, duration, and timing of Raman pulses, including the Bragg regime. The phase corrections caused by the finite pulses' durations are also calculated for the rectangular Raman pulse shape.

DOI: [10.1103/PhysRevA.108.063308](https://doi.org/10.1103/PhysRevA.108.063308)**I. INTRODUCTION**

Since its birth about 40 years ago [1], the field of atom interferometry has matured significantly. The current state and prospects in this area are presented, for example, in the reviews in [2–11] and the proposals in [12–21]. For the successful implementation of these programs, it is important to increase the phase of the atomic interferometer (AI), without enlarging the error of the phase measurement. Such an increase can be achieved by using AIs with a long interrogation time T and a large momentum transfer (LMT) during the interaction of an atom with pulses of optical fields. The highest value of $T = 1.15$ s was achieved [22] for freely falling atoms, while for atoms trapped in an optical lattice, the time between the first and last Raman pulses was increased to 1 min [23].

One may consider the nonlinear interaction of atoms with a resonant standing-wave pulse as the first implementation of the LMT technique. In this case, owing to the LMT, higher spatial harmonics of the atomic density arise [see Eq. (4) in [1]]. Various modifications of LMT used to produce such harmonics are briefly described in the Appendix.

Using the combination of adiabatic rapid passage and multiphoton Bragg diffraction allowed one to achieve an LMT of $5\hbar k$ [24], where $k = |\mathbf{k}|$, with \mathbf{k} the effective wave vector associated with the atomic beam splitter. The theory of multiphoton Bragg diffraction was developed and calculation of the phase of the AI at an LMT of $5\hbar k$ was implemented in the article [25]. It was shown [26] how the Bloch oscillation technique leads to an LMT beam splitter, and a beam splitter having an LMT of $5\hbar k$ was experimentally demonstrated. An efficient scheme based on fast adiabatic passage at an LMT of $10\hbar k$ was proposed in [27]. A Raman beam splitter, having an LMT of $16\hbar k$ [28], allowed one to increase the

recoil line splitting [29] by 15 times. Owing to the Bragg diffraction many times repeated, a beam splitter having an LMT of $45\hbar k$ [30] coherently splits the atomic cloud into two components separated from each other by a distance of 54 cm. In Ref. [31] a three-path AI with an LMT of $56\hbar k$ was created for precision measurements of the recoil frequency. Exploiting optical lattices as waveguides and beam splitters promises an LMT of $100\hbar k$ or more [32]. Instead of Bragg diffraction, one can use pulses of a traveling wave, resonant to the transition between the ground and metastable excited states. This approach was realized in Ref. [33], where an LMT of $146\hbar k$ was created. Twin-lattice atom interferometry leads to an LMT of $204\hbar k$ [34]. The combination of the fifth-order Bragg scattering and the pulse of the Bloch oscillations allowed one to increase the LMT to $405\hbar k$ [35]. Using the pulse of the Bloch oscillation [36], one achieved an LMT of $500\hbar k$ [37]. Owing to these achievements, currently, LMT is one of the promising methods for improving the accuracy of atomic navigators [38,39], gravimeters [40], and gyroscopes [41]. The results of the gravity acceleration and rotation rate measurements are summarized in Ref. [5].

A. Sequential large momentum transfer

One of the varieties of LMT is the sequential method, which uses a sequence of π pulses having opposite effective wave vectors. Sequential LMT (SLMT) was studied in Refs. [28,30,33], and in articles [30,33] SLMT was successfully used for the Mach-Zehnder AI (MZAI). One can use three types of beam splitters here: I, when the internal state of the atom stays the same during interaction with a pulse of a resonant optical field; II, when, during a one-photon transition, an atom is excited from the ground to a metastable excited state; and III, when the Raman pulse transfers the atom from one (ground) sublevel to another (excited) sublevel of the ground state.

^{*}Independent researcher, bdubetsky@gmail.com

In Ref. [1] the type-I beam splitter was a standing wave. Atom interference in the field of a standing wave was observed in Refs. [42,43]. In the Bragg regime, both a standing wave [44] and counterpropagating waves with a specially chosen frequency difference [30] can be used. Either a standing [1] or a traveling wave [45] was used as a type-II beam splitter. Type-II SLMT was observed in Ref. [33]. However, for most of the precision gravimeters and gyroscopes listed in the review in [5], Raman pulses, a type-III beam splitter, were used.

One can find a comparison of type-I and -III interferometers in Ref. [46], which considers the case when two atomic beam splitters having opposite effective wave vectors act simultaneously. This field configuration, the Raman standing wave, was proposed in Ref. [47]. It is now better known as the double-diffraction technique [48,49]. A further development of this approach, a combination of three Raman beam splitters, was proposed in Ref. [50].

For SLMT, it is important that under the action of a π pulse, the momentum of the atom does not change, or changes only by $\pm\hbar\mathbf{k}$. For a type-I splitter, this can only be achieved in the Bragg regime, when the small parameter of the problem is given by

$$\varepsilon = (\omega_k \tau)^{-1} \ll 1, \tag{1}$$

where τ is the pulse duration and

$$\omega_k = \frac{\hbar k^2}{2M} \tag{2}$$

is the recoil frequency, with M the mass of the atom. Since there are many π pulses in the SLMT, no matter how small the parameter (1) is, corrections to the atomic wave function, repeated many times, can lead to significant changes in the interference pattern. In the experiment [30]

$$\varepsilon \approx 0.18. \tag{3}$$

Unlike Ref. [51], we do not consider here issues related to frequency noise, or pulse fidelity. Even with beam splitters that are ideal in these respects, π pulses can be imperfect just because their duration is not long enough.

The disadvantage of type-III beam splitters, Raman pulses, are the ac Stark shifts of the atomic levels that do not coincide. On the other hand, SLMT can be realized for any value of ε . Raman pulses can have both long and short durations corresponding to the Bragg regime ($\varepsilon \ll 1$) and the opposite Raman-Nath regime

$$\varepsilon \gg 1. \tag{4}$$

In this article, we will consider SLMT with Raman pulses only. In this case, the MZAI scheme is shown in Fig. 1.

If the mirror pulse (second Raman pulse) is a resonant π pulse, then the atoms change their momenta and internal states with probability 1. In this case, the diagram has only two branches, red and blue. Atomic interference is the interference of the amplitudes of an atom in an excited state e , which arise when an atom moves along these branches. In this case, the contrast of the interference pattern is equal to 1. If the second pulse is not ideal, then the atoms do not change their state with a small amplitude (see the gray lines in the recoil diagram).

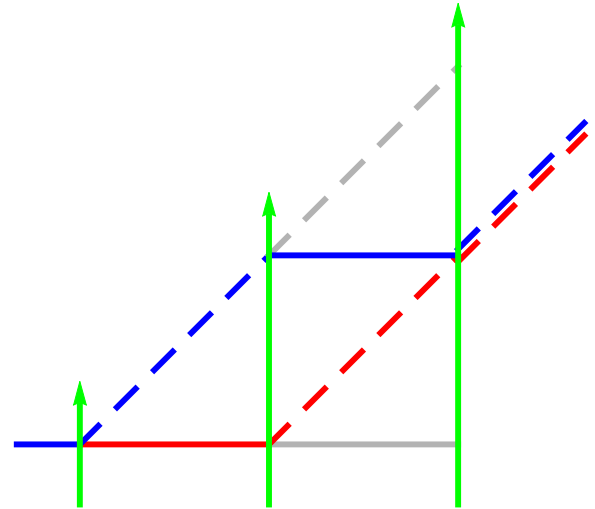


FIG. 1. Recoil diagram for the MZAI. Atoms in the ground and excited states are shown by solid and dashed lines, respectively.

Obviously, this only leads to a decrease in contrast and does not affect the phase of the MZAI.

The situation changes for SLMT, when in addition to the three main Raman pulses there are four sets of auxiliary π pulses, after the first, before and after the second, and before the third main pulses. Consider the simplest case, when each of the sets consists of only one π pulse (see Fig. 2).

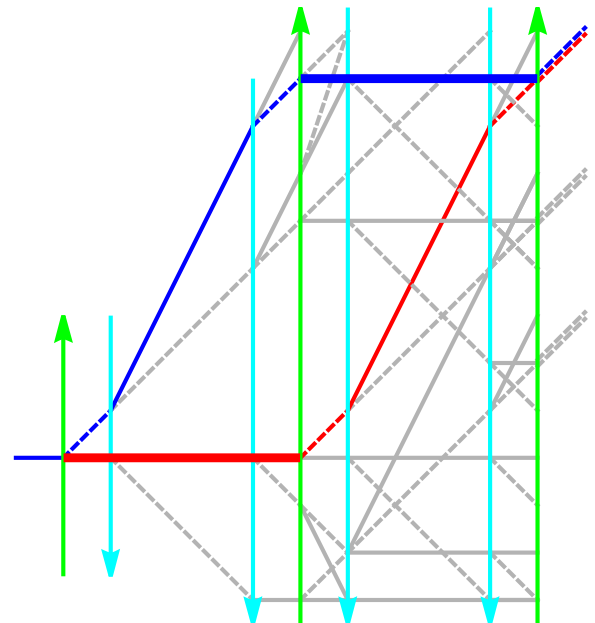


FIG. 2. SLMT. Each of the four sets of auxiliary pulses contains one π pulse. The main and auxiliary pulses are shown with green and cyan arrows, respectively. Thin, blue or red lines correspond to the resonant branches of the diagram, along which the momentum of the Raman field $\pm\hbar\mathbf{k}$ is transferred to the atom and the internal state of the atom changes. The thick horizontal lines correspond to the nonresonant branches of the diagram, along which the atoms remain in the ground state g and the momentum of the atom also does not change.

Each of the auxiliary pulses must satisfy the two requirements [30]: (i) It must be a resonant π pulse on the resonant branch of the recoil diagram and (ii) one has to choose the pulse parameters in such a way that the state of the unexcited atom on the other (nonresonant) branch remains unchanged. If both requirements are met exactly, then, by successively applying auxiliary pulses n times with alternative wave vectors $\pm\mathbf{k}$, one obtains a beam splitter with momentum transfer

$$\Delta\mathbf{p} = (n + 1)\hbar\mathbf{k}, \quad (5)$$

and the excitation probability of an atom in a uniform gravity field \mathbf{g} oscillates as

$$w = \frac{1}{2}[1 - \cos(\alpha + \phi_g)], \quad (6a)$$

$$\phi_g = (n + 1)\mathbf{k} \cdot \mathbf{g}T^2, \quad (6b)$$

where the parameter α , like the parameters α' and α'' below in Eqs. (8) and (14), are parts of the AI phase, independent of gravity.

In the Raman-Nath regime (4), when the pulse is so short that the violation of resonance conditions becomes insignificant, one can ignore both the first and the second requirements. In this case, the SLMT is twice as efficient, leading to the momentum transfer

$$\Delta\mathbf{p} = (2n + 1)\hbar\mathbf{k}. \quad (7)$$

The SLMT in the Raman-Nath approximation was observed in Ref. [33] for the one-photon transition. We are not aware of Raman beam splitters operating in the Raman-Nath regime (4).

Condition (ii) can be satisfied in the Bragg regime (1). In this case, if the Raman pulse is resonant to a transition along one of the branches, then it is not resonant for the other branch, and with accuracy (1) one can assume that the state of the atom remains unperturbed along the other branch. If the pulse is not perfect and the parameter ε is not small enough, then the pulse ceases to be a mirror, splits the states of the atom, and parasitic gray trajectories appear (see Figs. 1 and 2). One sees that, unlike the usual MZAI, in the MZAI with one auxiliary π pulse, parasitic trajectories lead to the appearance of parasitic interference ports, due to which a small addition to the signal (6) arises, which oscillates like

$$\Delta w = \beta \cos(\alpha' + \mathbf{k} \cdot \mathbf{g}T^2). \quad (8)$$

It should be emphasized that for precision measurements it is not enough that this correction be small; it is necessary that the amplitude of this correction be less than the accuracy of the MZAI phase measurement ϕ_{err} ,

$$|\beta| < \phi_{\text{err}}. \quad (9)$$

Only in this case does SLMT lead to progress in improving the accuracy of precision measurements. The error in the differential measurements of the MZAI phases was [52]

$$\phi_{\text{err}} \approx 2 \times 10^{-5} \text{ rad}. \quad (10)$$

One sees from Fig. 2 that parasitic ports are spatially separated from the main port by a distance

$$\Delta z = v_r T, \quad (11)$$

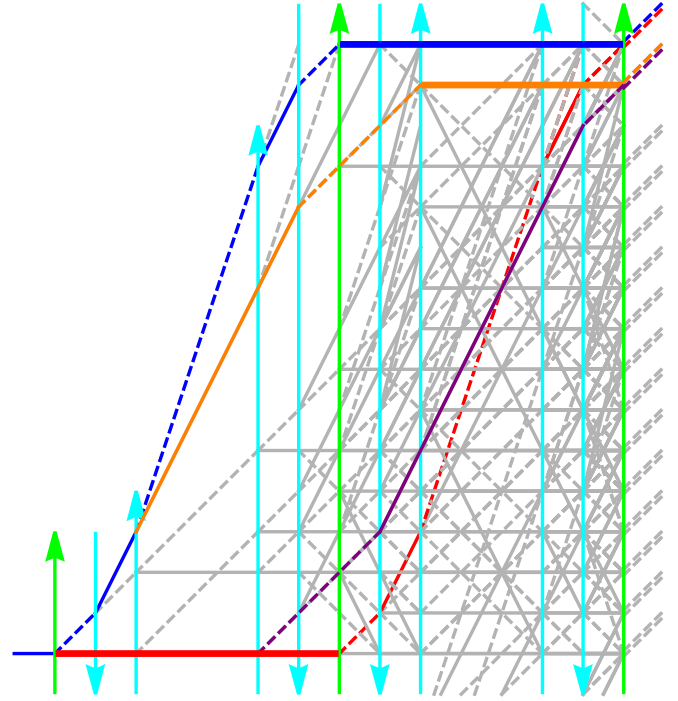


FIG. 3. Same as in Fig. 2 but for $n = 2$, when each set of auxiliary pulses contains two π pulses with opposite effective wave vectors. One included only color output ports in consideration.

where $v_r = |\mathbf{v}_r|$, with

$$\mathbf{v}_r = \frac{\hbar\mathbf{k}}{M} \quad (12)$$

the recoil velocity. Under the experimental conditions [30] $k = 1.61 \times 10^7 \text{ m}^{-1}$, $M = 87 \text{ a.u.}$, and $T = 1.04 \text{ s}$, the ports are separated from each other by a distance of $\Delta z = 1.2 \text{ cm}$. If, despite thermal expansion, the size of the atomic cloud, as well as the size of the detector, is less than Δz , then one can exclude the influence of parasitic ports.

The situation changes if several π pulses are used in each auxiliary set, $n > 1$. The case $n = 2$ is shown in Fig. 3. One sees that the distance between the main and parasitic ports decreases to the value

$$\Delta z = v_r d, \quad (13)$$

where d is the delay between adjacent auxiliary pulses. At $d = 200 \mu\text{s}$ [53], $\Delta z \approx 2.4 \mu\text{m}$. One may encounter technological difficulties in creating detectors and atomic clouds of such a small size. Otherwise, the ports overlap and parasitic signals occur. For example, a port caused by the interference of the blue-orange and red-purple branches (see Fig. 3) results in a parasitic signal

$$\Delta w = \beta \cos(\alpha'' + 2\mathbf{k} \cdot \mathbf{g}T^2). \quad (14)$$

With a larger number of auxiliary pulses, the role of parasitic terms can increase even more. Thus, for precision interferometry, it is necessary to use such beam splitters that satisfy requirements (i) and (ii) with the greatest accuracy. To satisfy requirement (i), it is enough to adjust the Raman frequency detuning of a given pulse to the frequency of the transition between the atomic momentum states before and

after the action of the field, while for requirement (ii) we propose in this paper to use Rabi oscillations [54] instead of the Bragg regime [30]. For the nonresonant branch, one can find such a pulse duration

$$\tau \sim \omega_k^{-1} \quad (15)$$

at which the probability of state splitting on this branch will be exactly 0. Below we find this duration for a rectangular Raman pulse and calculate the phase of the MZAI.

Since the pulse on the resonant branch must have an area π , the effective Rabi frequency Ω of a two-quantum transition between atomic states for auxiliary pulses may not coincide with the Rabi frequency for the main pulses. This, to a certain extent, is a technological challenge: the implementation of SLMT with sets of pulses having different intensities and durations. To circumvent this difficulty, we propose to use composite pulses [55], and we consider only noncontiguous composite pulses (NCPs) [56]. These pulses, as in Ref. [30], must be in resonance with atomic transitions $|\mathbf{p} + m\hbar\mathbf{k}\rangle \leftrightarrow |\mathbf{p} + (m-1)\hbar\mathbf{k}\rangle$, where $m > 1$ is an integer; their frequencies differ from the frequencies of the main pulses, resonant to transitions $|\mathbf{p}\rangle \leftrightarrow |\mathbf{p} + \hbar\mathbf{k}\rangle$, and they also differ from each other. However, the Rabi frequency for all pulses is the same and the sum of the pulse durations in a given NCP should be equal to 2τ , where τ is the duration of the first and third main $\frac{\pi}{2}$ pulses. If the composite pulse consists of two rectangular pulses, then each of them can have a duration τ .

Below we consider the NCP consisting of three rectangular pulses. If the durations of the first and third pulses coincide, then obviously the duration of each of the rectangular pulses can vary in the range $[0, \tau]$. Under the action of a composite pulse, the atom performs Rabi oscillations during each of the pulses and nutation of atomic coherence takes place in the time between rectangular pulses. Below we find such delay between pulses

$$\tau_b \sim \omega_k^{-1}, \quad (16)$$

under which, owing to a combination of nutation and Rabi oscillations, requirement (ii) is satisfied precisely.

B. Recoil phase

It is well known that atomic interference is caused by the quantization of the motion of the atomic center of mass. When the incident atomic momentum state $|\mathbf{p}\rangle$ splits into two states $|\mathbf{p}\rangle$ and $|\mathbf{p} + \hbar\mathbf{k}\rangle$ after passing through the beam splitter, the coherence between these states evolves as

$$\rho(\mathbf{p} + \hbar\mathbf{k}, \mathbf{p}, t) \propto \exp(-i\omega_{\mathbf{p}+\hbar\mathbf{k},\mathbf{p}}t), \quad (17)$$

where the frequency of transition between states

$$\omega_{\mathbf{p}+\hbar\mathbf{k},\mathbf{p}} = \frac{1}{2M\hbar}[(\mathbf{p} + \hbar\mathbf{k})^2 - \mathbf{p}^2] = \omega_D + \omega_k, \quad (18a)$$

$$\omega_D = \mathbf{k} \cdot \frac{\mathbf{p}}{M}, \quad (18b)$$

along with the Doppler frequency shift ω_D , contains a quantum term, the recoil frequency (2). If $t \sim T$ one can expect that the AI phase contains Doppler and quantum terms

$$\phi_D \sim \omega_D T, \quad (19a)$$

$$\phi_q \sim \omega_k T. \quad (19b)$$

Despite this, the phase of the well-known and widely used MZAI does not contain any quantum term in a uniform gravity field [see Eq. (6b) for $n = 0$]. The reason is that, although quantum corrections affect changes in the atom's coordinates at the moments of interaction with the second and third beam splitters, the corresponding quantum terms compensate each other in a uniform gravity field (see Appendix A in Ref. [57]). We would like to emphasize that the derivation of the expression for the AI phase is purely quantum (see examples of this derivation in Refs. [40,57,58]), but the result of these derivations, Eq. (6b), is purely classical. The absence of a quantum phase (19b) allows one to be in doubt that the MZAI phase is caused by the matter-wave interference (a sentiment held by the present author). Examples of the derivation of the expression for the phase without using the atomic center-of-mass motion quantization can be found in [59].

The quantum contribution arises in the rotating reference frame [60], in the nonuniform gravity field in the presence of the gravity-gradient tensor [61,62], in the presence of the gravity-gradient tensor of the second order [63], or in a strongly inhomogeneous source mass field [63]. The quantum term in the gravity-gradient field of the source mass was observed in [64] using the LMT method. In all these cases, the magnitude of the quantum terms is small compared to the phase ϕ_q in Eq. (19b). We predict here that the situation may change dramatically in the presence of auxiliary pulses. If the ultimate goal is not to create a high-precision gravimeter, but, as in [64], to observe the quantum term, and the timing of these pulses is comparable to the interrogation time T , then the quantum term turns out to be large and grows as $n/\ln n$ with increasing momentum transfer.

It should be noted, however, that the quantum term does not arise if, as in the experiments in [30,33,53], the auxiliary pulses are equidistant in time. With nonequidistant timing, the quantum term does not depend on the shape and duration of the pulse; it is the same for the rectangular pulses considered here, as well as in the Bragg regime [30]. However, for SLMT in the Raman-Nath approximation (4), for the both Raman beam splitters and atomic clocks [33], the quantum term must be recalculated.

C. Article structure

In this article, we use the Schrödinger equation in momentum space. In contrast to the same approach in Refs. [57,65], here we take into account the motion of the atom during the time of interaction with the pulse.

The overall plan of the paper is as follows. In the next section we use the solutions of the Schrödinger equation for the interaction of an atom with a rectangular pulse to determine the parameters of the NCPs, consisting of one, two, and three rectangular pulses. In Sec. III we calculate the MZAI phase. In Sec. IV we consider two types of quantum parts of MZAI phases. In Sec. V, an expression for the gravity part of the MZAI phase is obtained. We calculate the part of the gravity phase, independent of the duration of the main and auxiliary pulses, and corrections linear in these durations.

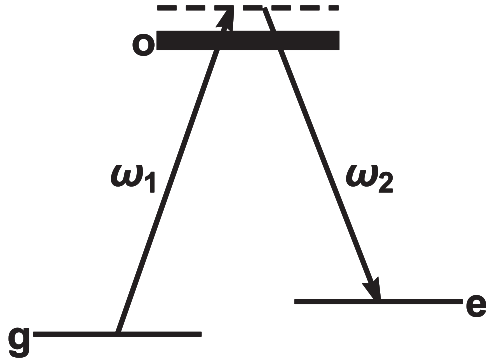


FIG. 4. Atomic level diagram.

II. MAIN RELATIONS

Let us consider the interaction of a three-level atom with the pulse of the field of two traveling waves resonant to adjacent atomic transitions

$$\mathbf{E}(\mathbf{x}, t) = (\mathbf{E}_1 \exp\{i[\mathbf{q}_1 \cdot \mathbf{x} - \omega_1 t - \phi_1(t)]\} + \mathbf{E}_2 \exp\{i[\mathbf{q}_2 \cdot \mathbf{x} - \omega_2 t - \phi_2(t)]\})f(t) + \text{c.c.}, \quad (20)$$

where \mathbf{E}_i , \mathbf{q}_i , ω_i , and $\phi_i(t)$ are the amplitudes, wave vectors, frequencies, and phases of the waves, respectively, and $f(t)$ is the shape of the pulse acting at the moment T and having a duration τ . We assume that the two atomic states $|g\rangle$ and

$|e\rangle$ are sublevels of the hyperfine structure of the ground-state manifold of the atom, while the third state $|o\rangle$ is a sublevel of the excited-state manifold; the fields \mathbf{E}_1 and \mathbf{E}_2 are resonant to the atomic transitions $g \rightarrow o$ and $e \rightarrow o$ (see Fig. 4). The location of the sublevels $|g\rangle$ and $|e\rangle$ on the atomic energy diagram is not important. However, we consider sublevels $|g\rangle$ and $|e\rangle$ to be ground and excited. The Hamiltonian of the interaction of an atom with a field is

$$H = \frac{p^2}{2M} - M\mathbf{g} \cdot \mathbf{x} + \frac{\hbar}{2}(\Omega_1 \exp\{i[\mathbf{q}_1 \cdot \mathbf{x} - \Delta_1 t - \phi_1(t)]\} \times |o\rangle\langle g| + \Omega_2 \exp\{i[\mathbf{q}_2 \cdot \mathbf{x} - \Delta_2 t - \phi_2(t)]\} \times |o\rangle\langle e| + \text{H.c.})f(t), \quad (21)$$

where \mathbf{p} is the momentum of the atom; \mathbf{g} is the gravity field;

$$\Omega_1 \equiv -2 \frac{\mathbf{d}_{og} \cdot \mathbf{E}_1}{\hbar}, \quad (22a)$$

$$\Omega_2 \equiv -2 \frac{\mathbf{d}_{oe} \cdot \mathbf{E}_2}{\hbar} \quad (22b)$$

are the Rabi frequencies of atomic transitions, with \mathbf{d} the dipole moment operator; and

$$\Delta_1 = \omega_1 - \omega_{og}, \quad (23a)$$

$$\Delta_2 = \omega_2 - \omega_{oe} \quad (23b)$$

are frequency detunings of the fields. The amplitudes of atomic levels evolve as

$$i\partial_t \tilde{a}(e, \mathbf{p}, t) = \left(\frac{p^2}{2M\hbar} - iM\mathbf{g} \cdot \partial_{\mathbf{p}} \right) \tilde{a}(e, \mathbf{p}, t) + \frac{\Omega_2^*}{2} \exp\{i[\Delta_2 t + \phi_2(t)]\} f(t) \tilde{a}(o, \mathbf{p} + \hbar\mathbf{q}_2, t), \quad (24a)$$

$$i\partial_t \tilde{a}(g, \mathbf{p}, t) = \left(\frac{p^2}{2M\hbar} - iM\mathbf{g} \cdot \partial_{\mathbf{p}} \right) \tilde{a}(g, \mathbf{p}, t) + \frac{\Omega_1^*}{2} \exp\{i[\Delta_1 t + \phi_1(t)]\} f(t) \tilde{a}(o, \mathbf{p} + \hbar\mathbf{q}_1, t), \quad (24b)$$

$$i\partial_t \tilde{a}(o, \mathbf{p}, t) = \left(\frac{p^2}{2M\hbar} - iM\mathbf{g} \cdot \partial_{\mathbf{p}} \right) \tilde{a}(o, \mathbf{p}, t) + \frac{\Omega_1}{2} \exp\{-i[\Delta_1 t + \phi_1(t)]\} f(t) \tilde{a}(g, \mathbf{p} - \hbar\mathbf{q}_1, t) + \frac{\Omega_2}{2} \exp\{-i[\Delta_2 t + \phi_2(t)]\} f(t) \tilde{a}(e, \mathbf{p} - \hbar\mathbf{q}_2, t). \quad (24c)$$

One assumes that the frequency detuning is large enough

$$\Delta_1 \approx \Delta_2 \approx \Delta, \quad (25a)$$

$$|\Delta| \gg \max\{|\tilde{\delta}|, \tau_f^{-1}, |\dot{\phi}_i|, |\mathbf{q}_i \cdot \mathbf{g}|T, |\omega_D|, \omega_k\}, \quad (25b)$$

where

$$\tilde{\delta} = \Delta_1 - \Delta_2 \quad (26)$$

is a Raman detuning and τ_f is the duration of the forward and backward fronts of the pulse. At this assumption one finds the expression for the level $|o\rangle$ amplitude [66]

$$\tilde{a}(o, \mathbf{p}, t) = \frac{f(t)}{2\Delta} (\Omega_1 \exp\{-i[\Delta_1 t + \phi_1(t)]\} \tilde{a}(g, \mathbf{p} - \hbar\mathbf{q}_1, t) + \Omega_2 \exp\{-i[\Delta_2 t + \phi_2(t)]\} \tilde{a}(e, \mathbf{p} - \hbar\mathbf{q}_2, t)). \quad (27)$$

Then for the amplitudes of the ground-state sublevels one gets

$$i\partial_t \tilde{a}(e, \mathbf{p}, t) = \left(\frac{p^2}{2M\hbar} - iM\mathbf{g} \cdot \partial_{\mathbf{p}} + \frac{|\Omega_2|^2}{4\Delta} \right) \tilde{a}(e, \mathbf{p}, t) + \frac{\Omega}{2} \exp\{-i[\tilde{\delta}t + \phi(t)]\} f^2(t) \tilde{a}(g, \mathbf{p} - \hbar\mathbf{k}, t), \quad (28a)$$

$$i\partial_t \tilde{a}(g, \mathbf{p}, t) = \left(\frac{p^2}{2M\hbar} - iM\mathbf{g} \cdot \partial_{\mathbf{p}} + \frac{|\Omega_1|^2}{4\Delta} \right) \tilde{a}(g, \mathbf{p}, t) + \frac{\Omega^*}{2} \exp\{i[\tilde{\delta}t + \phi(t)]\} f^2(t) \tilde{a}(e, \mathbf{p} + \hbar\mathbf{k}, t), \quad (28b)$$

where

$$\mathbf{k} = \mathbf{q}_1 - \mathbf{q}_2, \quad (29a)$$

$$\Omega = \frac{\Omega_1 \Omega_2^*}{2\Delta}, \quad (29b)$$

$$\phi(t) = \phi_1(t) - \phi_2(t) \quad (29c)$$

are the effective wave vector, the Rabi frequency, and the phase of the Raman beam splitter, respectively. Eliminating the ac Stark shift by a transformation to a rotating interaction picture, i.e., by introducing the amplitudes

$$\begin{pmatrix} \tilde{a}(e, \mathbf{p}, t) \\ \tilde{a}(g, \mathbf{p}, t) \end{pmatrix} = \exp \left[-\frac{i}{4\Delta} \int^t dt' \left(\frac{|\Omega_2|^2}{|\Omega_1|^2} \right) f^2(t') \right] \begin{pmatrix} a(e, \mathbf{p}, t) \\ a(g, \mathbf{p}, t) \end{pmatrix}, \quad (30)$$

one obtains

$$i \left(\partial_t + M\mathbf{g} \cdot \partial_{\mathbf{p}} + i \frac{p^2}{2M\hbar} \right) a(e, \mathbf{p}, t) = \frac{\Omega}{2} f^2(t) \exp[-i\delta t - i\phi(t)] a(g, \mathbf{p} - \hbar\mathbf{k}, t), \quad (31a)$$

$$i \left(\partial_t + M\mathbf{g} \cdot \partial_{\mathbf{p}} + i \frac{p^2}{2M\hbar} \right) a(g, \mathbf{p}, t) = \frac{\Omega^*}{2} f^2(t) \exp[i\delta t + i\phi(t)] a(e, \mathbf{p} + \hbar\mathbf{k}, t), \quad (31b)$$

where

$$\delta = \tilde{\delta} - \delta_S, \quad (32a)$$

$$\delta_S = \frac{|\Omega_2|^2 - |\Omega_1|^2}{4\Delta} \quad (32b)$$

is the ac Stark shift of the Raman line. The presence of an ac Stark shift would significantly complicate the present study. We will assume that this shift is absent. Experimental methods for eliminating the ac Stark shift were developed in Refs. [67,68]. If, for example, the Raman pulse has an area $\frac{\pi}{2}$, then from the equation $\delta_S = 0$ and Eq. (29b) one has

$$|\Omega_1| = \sqrt{\frac{\pi|\Delta|}{\tau}}. \quad (33)$$

At typical values of $\Delta = 2\pi \times 10$ GHz and $\tau = 30$ μ s, the parameter

$$|\Omega_1|/\Delta \approx 7 \times 10^{-4} \quad (34)$$

is small enough to neglect the ac Stark splitting of optical transitions $e \rightarrow o$ and $g \rightarrow o$ [69].

In an accelerated frame

$$\mathbf{p} = \mathbf{P} + M\mathbf{g}t, \quad (35)$$

using the atom's initial momentum \mathbf{P} as the independent variable, one gets

$$i \left(\frac{d}{dt} + i \frac{(\mathbf{P} + M\mathbf{g}t)^2}{2M\hbar} \right) a(e, \mathbf{P}, t) = \frac{\Omega}{2} f^2(t) \exp[-i\delta t - i\phi(t)] a(g, \mathbf{P} - \hbar\mathbf{k}, t), \quad (36a)$$

$$i \left(\frac{d}{dt} + i \frac{(\mathbf{P} + M\mathbf{g}t)^2}{2M\hbar} \right) a(g, \mathbf{P}, t) = \frac{\Omega^*}{2} f^2(t) \exp[i\delta t + i\phi(t)] a(e, \mathbf{P} + \hbar\mathbf{k}, t). \quad (36b)$$

Then one finds that in the interaction representation

$$a(n, \mathbf{P}, t) = \exp \left(-i \int_0^t dt' \frac{(\mathbf{P} + M\mathbf{g}t')^2}{2M\hbar} \right) c(n, \mathbf{P}, t) \quad (37)$$

the state vector

$$\underline{c}(\mathbf{P}, t) = \begin{pmatrix} c(e, \mathbf{P} + \frac{\hbar\mathbf{k}}{2}, t) \\ c(g, \mathbf{P} - \frac{\hbar\mathbf{k}}{2}, t) \end{pmatrix} \quad (38)$$

evolves as

$$i\dot{\underline{c}} = \frac{f^2(t)}{2} \begin{pmatrix} 0 & \Omega \exp\{-i[\delta t + \phi(t) - \mathbf{k} \cdot \frac{\mathbf{P}}{M}t - \frac{1}{2}\mathbf{k} \cdot \mathbf{g}t^2]\} \\ \Omega^* \exp\{i[\delta t + \phi(t) - \mathbf{k} \cdot \frac{\mathbf{P}}{M}t - \frac{1}{2}\mathbf{k} \cdot \mathbf{g}t^2]\} & 0 \end{pmatrix} \underline{c}. \quad (39)$$

One sees that in the accelerated frame the amplitude of the atomic state remains unchanged outside the field pulse

$$\underline{c}(\mathbf{P}, t) = \text{const at } t < T \text{ or } t > T + \tau. \quad (40)$$

If one chirps the field frequency linearly, i.e., if

$$\phi(t) = \phi + \alpha t^2/2, \quad (41)$$

and if the chirping rate α is close to $\mathbf{k} \cdot \mathbf{g}$,

$$|\alpha - \mathbf{k} \cdot \mathbf{g}| \tau^2 \ll 1, \quad (42)$$

then, considering Eq. (39) when

$$t = T + \varepsilon, \quad (43)$$

where

$$\varepsilon \sim \tau \ll T, \quad (44)$$

and neglecting terms quadratic in ε in the phase factors in Eq. (39), one arrives at the well-known equation for the amplitudes of a two-level atom interacting with the pulse of the field of arbitrary shape with constant frequency and phase

$$i\frac{d\underline{c}}{d\varepsilon} = \frac{f^2(T + \varepsilon)}{2} \begin{pmatrix} 0 & \Omega \exp\{-i[v\varepsilon + \phi(\mathbf{P})]\} \\ \Omega^* \exp\{i[v\varepsilon + \phi(\mathbf{P})]\} & 0 \end{pmatrix} \underline{c}, \quad (45)$$

where

$$v \equiv \delta(\mathbf{P}) = v^{(0)} + v^{(1)}, \quad (46a)$$

$$v^{(0)} \equiv \delta^{(0)}(\mathbf{P}) = \delta - \mathbf{k} \cdot \frac{\mathbf{P}}{M}, \quad (46b)$$

$$v^{(1)} = -(\mathbf{k} \cdot \mathbf{g} - \alpha)T, \quad (46c)$$

$$\phi(\mathbf{P}) = \phi + v^{(0)}T - \frac{1}{2}(\mathbf{k} \cdot \mathbf{g} - \alpha)T^2. \quad (46d)$$

After unitary transformation

$$\underline{c} = \underline{U}_\phi \tilde{\underline{c}}, \quad (47)$$

where the matrix \underline{U} is given by

$$\underline{U}_\phi = \begin{pmatrix} \exp[-\frac{i}{2}\phi(\mathbf{P})] & 0 \\ 0 & \exp[\frac{i}{2}\phi(\mathbf{P})] \end{pmatrix}, \quad (48)$$

one arrives at the phase-independent equation

$$i\frac{d\tilde{\underline{c}}}{d\varepsilon} = \frac{f^2(T + \varepsilon)}{2} \begin{pmatrix} 0 & \Omega \exp(-i v \varepsilon) \\ \Omega^* \exp(i v \varepsilon) & 0 \end{pmatrix} \tilde{\underline{c}}. \quad (49)$$

In the AI phase, the factor $\exp[\pm \frac{i}{2}\phi(\mathbf{P})]$ will be responsible for the Doppler and quantum phases (19), for the gravity phase (6b), and for the Ramsey phase

$$\phi_R \sim \delta T. \quad (50)$$

One might conclude that the results to be obtained below for the quantum, gravity, and Ramsey phases are independent of

the pulse shape $f(t)$ and do not change from the Raman-Nath regime (4) to the Bragg regime (1).

Consider now an NCP consisting of ℓ time-separated rectangular pulses

$$f(T + \varepsilon) = \begin{cases} 1 & \text{for } \varepsilon \in \bigcup_{m=1}^{\ell} (\tau_{0,m}, \tau_{0,m} + \tau_m) \\ 0 & \text{in other cases,} \end{cases} \quad (51)$$

where one turns on a pulse of duration τ_m at time $T + \tau_{0,m}$ so that

$$\tau_{0,m} = \sum_{m'=1}^{m-1} (\tau_{m'} + \tau_{bm'}), \quad (52)$$

where τ_{bm} is the delay time between adjacent pulses m and $m + 1$. After the next unitary transformation

$$\tilde{\underline{b}} = \underline{U}_\delta \underline{b}, \quad (53a)$$

$$\underline{U}_\delta = \begin{pmatrix} \exp(-\frac{i}{2}v\varepsilon) & 0 \\ 0 & \exp(\frac{i}{2}v\varepsilon) \end{pmatrix}, \quad (53b)$$

one finds

$$i\frac{d\underline{b}}{d\varepsilon} = \underline{h}\underline{b}, \quad (54a)$$

$$\underline{h} = \frac{1}{2} \begin{pmatrix} -v & \Omega \\ \Omega^* & +v \end{pmatrix}. \quad (54b)$$

The solution of this equation is well known. One can achieve it using composite rotation matrices. Alternatively, one can represent the \underline{h} matrix as

$$\underline{h} = \underline{\mathbf{h}} \cdot \underline{\sigma},$$

where

$$\underline{\mathbf{h}} = \frac{1}{2} \{\text{Re } \Omega, -\text{Im } \Omega, -v\}$$

and $\underline{\sigma} = \{\sigma_1, \sigma_2, \sigma_3\}$, with σ_i the Pauli matrix, and for the s matrix $\underline{\sigma} = \exp(-i\mathbf{h}t)$ use the expression [70]

$$\underline{f}(\underline{\mathbf{h}} \cdot \underline{\sigma}) = \frac{1}{2} \left(f(\underline{\mathbf{h}}) + f(-\underline{\mathbf{h}}) + \frac{\underline{\mathbf{h}} \cdot \underline{\sigma}}{h} [f(\underline{\mathbf{h}}) - f(-\underline{\mathbf{h}})] \right). \quad (55)$$

Immediately after the action of the pulse m , the wave function of the atom is

$$\underline{b}(T + \tau_{0,m} + \tau_m) = \underline{\sigma}(\tau_m) \underline{b}(T + \tau_{0,m}), \quad (56a)$$

$$\underline{\sigma}(\tau) = \begin{pmatrix} s_d(\tau) & -i s_a(\tau) \\ -i s_a^*(\tau) & s_d^*(\tau) \end{pmatrix}, \quad (56b)$$

$$s_d(\tau) = \cos \frac{\Omega_r \tau}{2} + i \frac{v}{\Omega_r} \sin \frac{\Omega_r \tau}{2}, \quad (56c)$$

$$s_a(\tau) = \frac{\Omega}{\Omega_r} \sin \frac{\Omega_r \tau}{2}, \quad (56d)$$

$$\Omega_r = \sqrt{|\Omega|^2 + v^2}. \quad (56e)$$

Hence, for $\Omega = 0$, corresponding to the time between pulses τ_{bm} , the s matrix is

$$\underline{s}_{bm} = \begin{pmatrix} \exp\left(\frac{i}{2}\nu\tau_{bm}\right) & 0 \\ 0 & \exp\left(-\frac{i}{2}\nu\tau_{bm}\right) \end{pmatrix}. \quad (57)$$

The numbering of auxiliary NCPs $\{\zeta, \beta\}$ will be introduced below in Sec. III, where we verify that either the pulse duration at $\ell = 1$ or the distance between pulses at $\ell > 1$ depends on the Raman detuning ν on the nonresonant branch of the

recoil diagram so that the total time of action of this NCP is a function of four parameters $\{\nu, \zeta, \beta, \ell\}$, for which one has

$$\tau(\nu, \zeta, \beta, \ell) = \tau_\ell + \sum_{m=1}^{\ell-1} (\tau_m + \tau_{bm}). \quad (58)$$

For the s matrix one has

$$\underline{s} = \underline{s}(\tau_\ell)\underline{s}_{b(\ell-1)}\underline{s}(\tau_{\ell-1})\cdots\underline{s}_{b1}\underline{s}(\tau_1). \quad (59)$$

Now, returning to the state vector (38) and to the laboratory frame,

$$\mathbf{P} = \mathbf{p}_{+, T+\tau(\nu, \zeta, \beta, \ell)}, \quad (60a)$$

$$\mathbf{p}_t \equiv \mathbf{p} - M\mathbf{g}t, \quad (60b)$$

one arrives at the next result

$$c(e, \mathbf{p}_+, T + \tau(\nu, \zeta, \beta, \ell)) = S_{ee}\left(\mathbf{p}_{+, T+\tau(\nu, \zeta, \beta, \ell)} - \frac{\hbar\mathbf{k}}{2}\right)c(e, \mathbf{p}_-, T) + S_{eg}\left(\mathbf{p}_{+, T+\tau(\nu, \zeta, \beta, \ell)} - \frac{\hbar\mathbf{k}}{2}\right)c(g, \mathbf{p}_- - \hbar\mathbf{k}, T), \quad (61a)$$

$$c(g, \mathbf{p}_+, T + \tau(\nu, \zeta, \beta, \ell)) = S_{ge}\left(\mathbf{p}_{+, T+\tau(\nu, \zeta, \beta, \ell)} + \frac{\hbar\mathbf{k}}{2}\right)c(e, \mathbf{p}_- + \hbar\mathbf{k}, T) + S_{gg}\left(\mathbf{p}_{+, T+\tau(\nu, \zeta, \beta, \ell)} + \frac{\hbar\mathbf{k}}{2}\right)c(g, \mathbf{p}_-, T), \quad (61b)$$

where

$$S(\mathbf{P}) = \begin{pmatrix} \hat{s}_{ee} & \exp[-i\phi(\mathbf{P})]\hat{s}_{eg} \\ \exp[i\phi(\mathbf{P})]\hat{s}_{ge} & \hat{s}_{gg} \end{pmatrix}, \quad (62a)$$

$$\hat{s} = \begin{pmatrix} \exp\left[-\frac{i}{2}\nu\tau(\nu, \zeta, \beta, \ell)\right]s_{ee} & \exp\left[-\frac{i}{2}\nu\tau(\nu, \zeta, \beta, \ell)\right]s_{eg} \\ \exp\left[\frac{i}{2}\nu\tau(\nu, \zeta, \beta, \ell)\right]s_{ge} & \exp\left[\frac{i}{2}\nu\tau(\nu, \zeta, \beta, \ell)\right]s_{gg} \end{pmatrix}, \quad (62b)$$

where $s_{\alpha\beta}$ is a matrix element of the s matrix (59).

The momentum of the atom changes due to the transfer of the momentum of the photon $\pm\hbar\mathbf{k}$ and under the action of gravitation \mathbf{g} . The change in the momentum of the atom under the action of a uniform gravitational field does not depend on the initial value of the momentum [see Eq. (60b)] and therefore does not depend on the momentum of the photon transferred to the atom. This allows one to represent the momenta of an atom as

$$\mathbf{p}_\pm = \mathbf{p}'_\pm + \mathfrak{N}\hbar\mathbf{k}, \quad (63)$$

where \mathfrak{N} is the total number of photon momenta transferred to the atom at a given point in the recoil diagram. Below we omit the prime in the expressions for momenta. If the effective wave vector of a given NCP is equal to $\pm\mathbf{k}$, then, keeping in mind the redefinition (63), one obtains, instead of Eqs. (61),

$$c(e, \mathbf{p}_+ + \mathfrak{N}\hbar\mathbf{k}, T + \tau(\nu, \zeta, \beta, \ell)) = S_{ee}\left(\mathbf{p}_{+, T+\tau(\nu, \zeta, \beta, \ell)} + (2\mathfrak{N} \mp 1)\frac{\hbar\mathbf{k}}{2}\right)c(e, \mathbf{p}_- + \mathfrak{N}\hbar\mathbf{k}, T) \\ + S_{eg}\left(\mathbf{p}_{+, T+\tau(\nu, \zeta, \beta, \ell)} + (2\mathfrak{N} \mp 1)\frac{\hbar\mathbf{k}}{2}\right)c(g, \mathbf{p}_- + (\mathfrak{N} \mp 1)\hbar\mathbf{k}, T), \quad (64a)$$

$$c(g, \mathbf{p}_+ + \mathfrak{N}\hbar\mathbf{k}, T + \tau(\nu, \zeta, \beta, \ell)) = S_{ge}\left(\mathbf{p}_{+, T+\tau(\nu, \zeta, \beta, \ell)} + (2\mathfrak{N} \pm 1)\frac{\hbar\mathbf{k}}{2}\right)c(e, \mathbf{p}_- + (\mathfrak{N} \pm 1)\hbar\mathbf{k}, T) \\ + S_{gg}\left(\mathbf{p}_{+, T+\tau(\nu, \zeta, \beta, \ell)} + (2\mathfrak{N} \pm 1)\frac{\hbar\mathbf{k}}{2}\right)c(g, \mathbf{p}_- + \mathfrak{N}\hbar\mathbf{k}, T). \quad (64b)$$

The independent variable is the momentum of the atom after interaction with the NCP, \mathbf{p}_+ . Then from Eqs. (60) it follows that the momentum of the atom before this interaction is

$$\mathbf{p}_- = \mathbf{p}_{+, \tau(\nu, \zeta, \beta, \ell)}. \quad (65)$$

One thus takes into account that during the interaction with the NCP, the atom was accelerated, i.e. before interaction with a given NCP having a duration τ , the momentum of the atom \mathbf{p}_- was smaller by $M\mathbf{g}\tau$ than the momentum after the interaction \mathbf{p}_+ .

If the NCP $\{\zeta, \beta\}$ follows the NCP $\{\zeta', \beta'\}$, then it follows from Eq. (40) that

$$\underline{c}(\mathbf{p}_-^{(\zeta, \beta)}, T_{\zeta, \beta}) = \underline{c}(\mathbf{p}_+^{(\zeta', \beta')}, T_{\zeta', \beta'} + \tau(v', \zeta', \beta', \ell')), \quad (66a)$$

$$\mathbf{p}_+^{(\zeta', \beta')} = \mathbf{p}_-^{(\zeta, \beta)} - T_{\zeta, \beta} - T_{\zeta', \beta'} - \tau(v', \zeta', \beta', \ell'), \quad (66b)$$

where $T_{\zeta, \beta}$ is the moment of action of the NCP $\{\zeta, \beta\}$, $\mathbf{p}_\pm^{(\zeta, \beta)}$ is the atomic momentum before and after the action of this NCP, and $\tau(v', \zeta', \beta', \ell')$ is the duration (58) of the NCP $\{\zeta', \beta'\}$.

Equations (66) mean that atomic state \underline{c} stays unchanged between NCPs and only atomic momentum changes owing to gravity.

Knowing \mathbf{p}_+ , one can restore the momenta of atoms before and after the action of all preceding NCPs applying consequently Eqs. (65) and (66b).

We have not been able to construct an NCP that satisfies requirement (ii) for an arbitrary ℓ . We have done this only for the simplest cases $\ell = 1, 2$, and 3 . Let us consider these cases separately.

A. Case $\ell = 1$

In this case, $\underline{s} = \underline{\sigma}(\tau)$, where τ is the duration of the NCP and $\underline{\sigma}(\tau)$ is given in Eqs. (56). In Eqs. (46) Raman frequency detuning consists of two terms $\nu^{(0)}$ and $\nu^{(1)}$. The contribution to the s matrix (56b) from the term $\nu^{(1)}$ can be estimated as

$$\delta \underline{s} = \underline{s}' \nu^{(1)} \sim (\mathbf{k} \cdot \mathbf{g} - \alpha) T \tau, \quad (67)$$

where

$$\underline{s}' \equiv \partial \underline{s} / \partial \nu \quad (68)$$

and we take into account that the characteristic size of the s -matrix dependence on ν is of the order of τ^{-1} . The parameter $(\mathbf{k} \cdot \mathbf{g} - \alpha) T \tau$ is responsible for the corrections to the MZAI phase caused by the finite duration of the Raman pulses [71–73]. We consider this parameter to be small,

$$\delta \phi \sim |\mathbf{k} \cdot \mathbf{g} - \alpha| T \tau \ll 1, \quad (69)$$

and calculate the MZAI phase up to a correction linear in τ .

Here and below we reserve the denotations ν and ν_r for the Raman frequency detuning on the nonresonant and resonant branches of the recoil diagram, respectively. The effective Rabi frequency

$$|\Omega| = \frac{\pi}{\tau}. \quad (70)$$

Let us first consider the nonresonant branch of the recoil diagram. In the zero approximation in $\delta \phi$ we are looking for such a duration τ of the auxiliary Raman pulse at which the atom does not change its state with a probability of 100%,

$$|s_{gg}| = 1. \quad (71)$$

From Eq. (56c) the solution to this equation is

$$\Omega_r \tau = 2j\pi, \quad (72)$$

where j is an arbitrary positive integer. From Eqs. (70) and (72) one finds that

$$\tau = \pi \frac{\sqrt{4j^2 - 1}}{|\nu^{(0)}|}. \quad (73)$$

In this case, the s matrix is

$$\underline{\sigma}(\tau) = (-1)^j I, \quad (74)$$

where I is the identity matrix. Consider now the amendments (67). Since

$$s'_d = -\frac{\nu \tau}{2\Omega_r} \sin \frac{\Omega_r \tau}{2} + i \left(\frac{1}{\Omega_r} \sin \frac{\Omega_r \tau}{2} + \frac{\nu^2 \tau}{2\Omega_r^2} \cos \frac{\Omega_r \tau}{2} - \frac{\nu^2}{\Omega_r^3} \sin \frac{\Omega_r \tau}{2} \right), \quad (75a)$$

$$s'_a = \frac{\Omega \nu}{\Omega_r} \left(-\frac{1}{\Omega_r^2} \sin \frac{\Omega_r \tau}{2} + \frac{\tau}{2\Omega_r} \cos \frac{\Omega_r \tau}{2} \right). \quad (75b)$$

Then from Eqs. (70) and (72) one gets that, taking into account corrections linear in τ , the s matrix is

$$\underline{s} = \begin{pmatrix} \exp \{i[\eta_0^{(1)} - \eta_1^{(1)}(\nu)v^{(1)}]\} & -i(-1)^j [\pi \Omega (4j^2 - 1) / 8j^2 |\Omega| \nu] v^{(1)} \\ -i(-1)^j [\pi \Omega^* (4j^2 - 1) / 8j^2 |\Omega| \nu] v^{(1)} & \exp \{i[\eta_0^{(1)} + \eta_1^{(1)}(\nu)v^{(1)}]\} \end{pmatrix}, \quad (76a)$$

$$\eta_0^{(1)} = j\pi, \quad (76b)$$

$$\eta_1^{(1)}(\nu) = -\frac{\pi(4j^2 - 1)^{3/2}}{8j^2 |\nu|}. \quad (76c)$$

One sees that the correction (46c) due to the small but nonzero pulse duration results in small off-diagonal s -matrix elements. This means that even an ideal rectangular pulse leads to a small splitting of the atomic state on the nonresonant branch of the recoil diagram. In the following, we will only take into account the influence of corrections (46c) on the AI phase and therefore we will neglect the off-diagonal elements of the s matrix (76a).

Let us now turn to the resonance branch. Here the π pulse must, with 100% probability, transfer the atom from one internal state to another while transmitting the momentum $\pm \hbar \mathbf{k}$. However, at $\nu = 0$, from Eqs. (75), derivatives $\{s'_d, s'_a\} = \{i\frac{\pi}{\tau}, 0\}$ so that

$$\underline{s} = \begin{pmatrix} i\tau \nu_r^{(1)} / \pi & -i \exp(i \arg \Omega) \\ -i \exp(-i \arg \Omega) & -i\tau \nu_r^{(1)} / \pi \end{pmatrix}. \quad (77)$$

One sees that the mirror, the resonant π pulse, ceases to be ideal owing to the finite duration of the pulse. With a small amplitude linear in this duration, the momentum of the atom and its internal state remain unchanged. The diagonal elements of the s matrix (77) do not affect the phase of the MZAI and we neglect them below.

B. Case $\ell = 2$

We have already noted that the disadvantage of a single Raman pulse is that for each new value of the Raman detuning $\nu^{(0)}$ one must change the pulse duration according to Eq. (73) and then change the Rabi frequency according to Eq. (70). For $\ell > 1$ we will consider NCPs, in which the Rabi frequency is the same as that of the main pulses, and for given durations of rectangular pulses τ_m ($m = 1, \dots, \ell$), condition (ii) is reached owing to properly chosen time delays between pulses τ_{bm} ($m = 1, \dots, \ell - 1$). Here and below we reserve the denotation τ only for the duration of the first main $\frac{\pi}{2}$ pulse, so for all pulses the magnitude of the Rabi frequency is

$$|\Omega| = \frac{\pi}{2\tau}. \quad (78)$$

1. Resonant branch $\nu_r^{(0)} = 0$

For the s matrix (57) one obtains

$$s_{bm} = I + \frac{i}{2} \nu^{(1)} \tau_{bm} \underline{\sigma}_3, \quad (79)$$

2. Nonresonant branch

In this case one will get for the s matrix (59)

$$\underline{s} = \underline{\sigma}(\tau) s_{b1} \underline{\sigma}(\tau), \quad (86)$$

where $\underline{\sigma}(\tau)$ and s_{b1} are given by Eqs. (56) and (57). Multiplying the matrices, one gets

$$\underline{s} = \begin{pmatrix} \exp\left(\frac{i}{2}\nu\tau_b\right)s_d^2 - \exp\left(-\frac{i}{2}\nu\tau_b\right)|s_a|^2 & -i \exp\left(\frac{i}{2}\nu\tau_b\right)s_a s_d - i \exp\left(-\frac{i}{2}\nu\tau_b\right)s_a s_d^* \\ -i \exp\left(\frac{i}{2}\nu\tau_b\right)s_a^* s_d - i \exp\left(-\frac{i}{2}\nu\tau_b\right)s_a^* s_d^* & \exp\left(-\frac{i}{2}\nu\tau_b\right)s_d^{*2} - \exp\left(\frac{i}{2}\nu\tau_b\right)|s_a|^2 \end{pmatrix}. \quad (87)$$

One sees that for equal durations τ_1 and τ_2 ,

$$s_{ee} = s_{gg}^*, \quad (88a)$$

$$s_{ge} = \exp(-2i \arg \Omega) s_{eg}. \quad (88b)$$

Condition (ii) is satisfied if the delay between pulses, τ_b , is the root of the equation

$$s_{eg} = 0. \quad (89)$$

Subject to Eq. (78), one gets

$$\tau_b = \tau^{(2)}(j, \nu) = \frac{1}{\nu} \left[-2 \arctan \left(\frac{2\nu\tau}{\sqrt{\pi^2 + 4\nu^2\tau^2}} \tan \frac{1}{4} \sqrt{\pi^2 + 4\nu^2\tau^2} \right) + \text{sgn}(\nu)(2j+1)\pi \right]. \quad (90)$$

Since $\tau_b > 0$, then j must be a non-negative integer.

In contrast to the SLMT in the Bragg regime [30], in our case, although the NCP does not excite the atom and does not change its momentum, it leads to the appearance of a phase factor in the atomic wave function. From Eqs. (87) and (90) one will get for

where $\underline{\sigma}_3$ is the Pauli matrix. Then

$$\underline{s} = \underline{\sigma} \left(\sum_{m=1}^{\ell} \tau_m \right) + \delta s_b, \quad (80a)$$

$$\delta s_b = \frac{i}{2} \nu^{(1)} \sum_{m=1}^{\ell-1} \tau_{bm} \underline{\sigma} \left(\sum_{m'=m+1}^{\ell} \tau_{m'} \right) \underline{\sigma}_3 \underline{\sigma} \left(\sum_{m'=1}^m \tau_{m'} \right). \quad (80b)$$

Here we have used the law of multiplication for s matrices,

$$\underline{\sigma}(\tau_m) \underline{\sigma}(\tau_{m-1}) = \underline{\sigma}(\tau_m + \tau_{m-1}). \quad (81)$$

In order for the NCP to be a π pulse, it is necessary that the sum of durations τ_m be equal to 2τ ,

$$\sum_{m=1}^{\ell} \tau_m = 2\tau. \quad (82)$$

Then, after the change $\tau \rightarrow 2\tau$ in Eq. (77), one will obtain

$$\underline{\sigma}(2\tau) = \begin{pmatrix} 2i\tau \nu_r^{(1)}/\pi & -i \exp(i \arg \Omega) \\ -i \exp(-i \arg \Omega) & -2i\tau \nu_r^{(1)}/\pi \end{pmatrix}. \quad (83)$$

For $\ell = 2$ we have considered only the symmetric case, when two rectangular pulses have the same duration

$$\tau_1 = \tau_2 = \tau \quad (84)$$

when $\delta s_b = \frac{i}{2} \nu^{(1)} \tau_b \underline{\sigma}_3$, with $\tau_b \equiv \tau_{b1}$, and therefore

$$\underline{s} = \begin{pmatrix} i(2\tau/\pi + \tau_b/2)\nu_r^{(1)} & -i \exp(i \arg \Omega) \\ -i \exp(-i \arg \Omega) & -i(2\tau/\pi + \tau_b/2)\nu_r^{(1)} \end{pmatrix}. \quad (85)$$

this factor

$$s_{gg} = \exp \{i[\eta_0^{(2)} + \eta_0^{(2)}(v)]\}, \quad (91a)$$

$$\eta_0^{(2)} = \left[j - \frac{1}{2} \operatorname{sgn}(v) \right] \pi, \quad (91b)$$

$$\eta_0^{(2)}(v) = -\arctan \left[\frac{2v\tau}{\sqrt{\pi^2 + 4v^2\tau^2}} \tan \left(\frac{1}{4} \sqrt{\pi^2 + 4v^2\tau^2} \right) \right]. \quad (91c)$$

Let us now turn to the calculation of the correction (67). Direct calculation of the derivative (68) turned out to be unproductive. Note, however, that the s matrix is a function of two variables v and τ_b and therefore

$$\frac{d}{dv} \underline{s} |_{\tau_b = \tau^{(2)}(j, v)} = \underline{s}' + \frac{\partial \underline{s}}{\partial \tau_b} \Big|_{\tau_b = \tau^{(2)}(j, v)} \frac{d\tau^{(2)}(j, v)}{dv}. \quad (92)$$

From Eqs. (91a), (90), and (87) it follows, correspondingly, that

$$\frac{d}{dv} s_{gg} |_{\tau_b = \tau^{(2)}(j, v)} = -i s_{gg} \operatorname{Im} \frac{s'_d}{s_d}, \quad (93a)$$

$$\frac{d\tau^{(2)}(j, v)}{dv} = -\frac{1}{v} \tau^{(2)}(j, v) - \frac{2}{v} \operatorname{Im} \left(\frac{s'_d}{s_d} \right), \quad (93b)$$

$$\frac{\partial s_{gg}}{\partial \tau_b} \Big|_{\tau_b = \tau^{(2)}(j, v)} = \frac{i}{2} v s_{gg} (|s_a|^2 - |s_d|^2), \quad (93c)$$

and substituting these values into Eq. (92), one calculates consequently s'_{gg} and δs_{gg} . The correction δs_{gg} is calculated in a similar way. As a result, taking into account Eqs. (88), one arrives at the following expression for the s matrix:

$$\underline{s} = \begin{pmatrix} \exp \{ -i[\eta_0^{(2)} + \eta_0^{(2)}(v^{(0)}) + \eta_1^{(2)}(v^{(0)})v^{(1)}] \} & -(-1)^j \operatorname{sgn}(v^{(0)}) s_a |s_d| [\tau_b + 2 \operatorname{Im} \left(\frac{s'_d}{s_d} \right)] v^{(1)} \\ -(-1)^j \operatorname{sgn}(v^{(0)}) s_a^* |s_d| [\tau_b + 2 \operatorname{Im} \left(\frac{s'_d}{s_d} \right)] v^{(1)} & \exp \{ i[\eta_0^{(2)} + \eta_0^{(2)}(v^{(0)}) + \eta_1^{(2)}(v^{(0)})v^{(1)}] \} \end{pmatrix}, \quad (94a)$$

$$\eta_1^{(2)}(v) = -\frac{\tau^{(2)}(j, v)}{2} (|s_d|^2 - |s_a|^2) - 2|s_d|^2 \operatorname{Im} \frac{s'_d}{s_d}. \quad (94b)$$

As in the preceding section, we will further neglect the diagonal elements of the resonant s matrix (85) and the off-diagonal elements of the nonresonant s matrix (94a).

C. Case $\ell = 3$

Here we also consider only the symmetric case, when

$$\tau_3 = \tau_1, \quad (95a)$$

$$\tau_2 = 2(\tau - \tau_1), \quad (95b)$$

$$\tau_{b1} = \tau_{b2} \equiv \tau_b. \quad (95c)$$

1. Resonant branch $v_r^{(0)} = 0$

Here the σ matrix is given in Eq. (83). Then, computing the matrix (80b) using Eqs. (56c), (56d), and (95), one arrives at the following expression for the resonant s matrix:

$$\underline{s} = \begin{pmatrix} i v_r^{(1)} \{ \tau_b \cos \left[\frac{\pi}{2} \left(1 - \frac{\tau_1}{\tau} \right) \right] + 2 \frac{\tau}{\pi} \} & -i \exp(i \arg \Omega) \\ -i \exp(-i \arg \Omega) & -i v_r^{(1)} \{ \tau_b \cos \left[\frac{\pi}{2} \left(1 - \frac{\tau_1}{\tau} \right) \right] + 2 \frac{\tau}{\pi} \} \end{pmatrix}. \quad (96)$$

2. Nonresonant branch

In this case, the s matrix (59) is given by

$$\underline{s} = \underline{\sigma}(\tau_1) \underline{s}_b \underline{\sigma}(\tau_2) \underline{s}_b \underline{\sigma}(\tau_1), \quad (97)$$

where $\underline{\sigma}(\tau)$ and \underline{s}_b are given by Eqs. (56) and (57). Taking into account the fact that the effective Rabi frequency Ω does not change for all components of the symmetric NCP of rectangular pulses and multiplying the matrices in Eq. (97), one arrives at

the result

$$\underline{s} = \begin{pmatrix} \exp(i\nu\tau_b)s_{d1}^2s_{d2} - \exp(-i\nu\tau_b)|s_{a1}|^2s_{d2}^* - 2s_{d1}|s_{a2}s_{a1}| & -i\{2s_{a1}\operatorname{Re}[\exp(i\nu\tau_b)s_{d1}s_{d2}] + s_{a2}(|s_{d1}|^2 - |s_{a1}|^2)\} \\ -i\{s_{a1}^*2\operatorname{Re}[\exp(i\nu\tau_b)s_{d2}s_{d1}] + s_{a2}^*(|s_{d1}|^2 - |s_{a1}|^2)\} & \exp(-i\nu\tau_b)s_{d1}^*s_{d2}^* - \exp(i\nu\tau_b)s_{d2}|s_{a1}|^2 - 2s_{d1}^*|s_{a2}s_{a1}| \end{pmatrix}, \quad (98)$$

where

$$s_{di} = s_d(\tau_i), \quad (99a)$$

$$s_{ai} = s_a(\tau_i). \quad (99b)$$

If one chooses the delay between rectangular pulses, τ_b , in such a way that

$$\cos[\nu\tau_b + \arg(s_{d1}s_{d2})] = \frac{|s_{a2}|(|s_{a1}|^2 - |s_{d1}|^2)}{2|s_{a1}s_{d1}s_{d2}|}, \quad (100)$$

then $s_{eg} = 0$ and therefore the NCP satisfies requirement (ii). Figure 5 shows (in gray) the range for which Eq. (100) has a solution.

The solution of the Eq. (100) is given by

$$\tau_b = \frac{1}{2}\tau^{(3\pm)}(j, \nu), \quad (101a)$$

$$\tau^{(3\pm)}(j, \nu) = \frac{2}{\nu} \left(\pm \arccos \frac{|s_{a2}|(|s_{a1}|^2 - |s_{d1}|^2)}{2|s_{a1}s_{d1}s_{d2}|} - \arctan \frac{\operatorname{Im}(s_{d1}s_{d2})}{\operatorname{Re}(s_{d1}s_{d2})} + 2j\pi \right), \quad (101b)$$

where for each value of ν the integer j can take only those values for which $\tau_b > 0$. Hence, the wave function of the atom in the ground state, after the action of the NCP, acquires the phase factor

$$s_{gg} = \exp[i\eta_0^{(3\pm)} + i\eta_0^{(3\pm)}(\nu)], \quad (102a)$$

$$\eta_0^{(3\pm)} = \pi, \quad (102b)$$

$$\eta_0^{(3\pm)}(\nu) = -\arctan \left(\frac{2\nu}{\sqrt{\pi^2 + 4\nu^2\tau^2}} \tan \frac{\tau_1}{4\tau} \sqrt{\pi^2 + 4\nu^2\tau^2} \right) \pm \arccos \frac{1}{2} \left| \frac{s_{a2}}{s_{a1}s_{d1}} \right|. \quad (102c)$$

To calculate linear in $\nu^{(1)}$ corrections, one can use the equality (92), in which one should make the substitution

$$\tau^{(2)}(j, \nu) \rightarrow \frac{1}{2}\tau^{(3\pm)}(j, \nu). \quad (103)$$

From Eqs. (102a) and (98) it follows that

$$\frac{d}{d\nu} s_{gg}|_{\tau_b=0.5\tau^{(3\pm)}(j, \nu)} = i \frac{d\eta_0^{(3\pm)}(\nu)}{d\nu} s_{gg}|_{\tau_b=0.5\tau^{(3\pm)}(j, \nu)}, \quad (104a)$$

$$\left. \frac{\partial s_{gg}}{\partial \tau_b} \right|_{\tau_b=0.5\tau^{(3\pm)}(j, \nu)} = i\nu(|s_{a1}|^2 - |s_{d1}|^2) s_{gg}|_{\tau_b=0.5\tau^{(3\pm)}(j, \nu)}, \quad (104b)$$

respectively. These expressions allow one to extract s'_{gg} from Eq. (92) [taking into account the replacement (103)] and get δs_{gg} . Computing the off-diagonal element s_{eg} in a similar way, one arrives at the result

$$\underline{s} = \begin{pmatrix} \exp[-i\eta_0^{(3\pm)} - i\eta_0^{(3\pm)}(\nu) - i\eta_1^{(3\pm)}(\nu)\nu_1] & \mp i \exp(i \arg \Omega) \frac{d\tau^{(3\pm)}}{d\nu} \sqrt{4|s_{a1}|^2|s_{d1}|^2 - |s_{a2}|^2\nu^{(0)}\nu^{(1)}} \\ \mp i \exp(-i \arg \Omega) \frac{d\tau^{(3\pm)}}{d\nu} \sqrt{4|s_{a1}|^2|s_{d1}|^2 - |s_{a2}|^2\nu^{(0)}\nu^{(1)}} & \exp[i\eta_0^{(3\pm)} + i\eta_0^{(3\pm)}(\nu) + i\eta_1^{(3\pm)}(\nu)\nu_1] \end{pmatrix}, \quad (105a)$$

$$\eta_1^{(3\pm)}(\nu) = \frac{d\eta_0^{(3\pm)}(\nu)}{d\nu} - \frac{\nu}{2}(|s_{a1}|^2 - |s_{d1}|^2) \frac{d\tau^{(3\pm)}(j, \nu)}{d\nu}. \quad (105b)$$

From Eqs. (58) and (73) the total NCP duration is given by

$$\tau(\nu, \zeta, \beta, 1) = \pi \frac{\sqrt{4j_{\zeta, \beta, 1}^2 - 1}}{|\nu|}, \quad (106a)$$

$$\tau(\nu, \zeta, \beta, 2) = 2\tau + \tau^{(2)}(j_{\zeta, \beta, 2}, \nu), \quad (106b)$$

$$\tau(\nu, \zeta, \beta, 3_{\pm}) = 2\tau + \tau^{(3\pm)}(j_{\zeta, \beta, 3_{\pm}}, \nu), \quad (106c)$$

with $\tau^{(2)}(j, \nu)$ and $\tau^{(3\pm)}(j, \nu)$ given in Eqs. (90) and (101b), respectively.

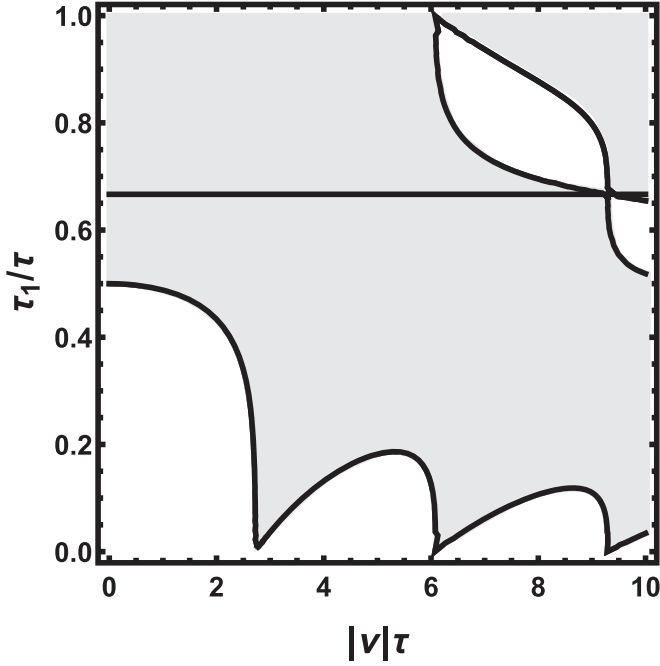


FIG. 5. For a given value of the Raman detuning ν , the duration of the first and third rectangular pulses should be in the gray area. The straight line corresponds to pulses of equal duration, $\tau_1 = \tau_2 = \tau_3 = \frac{2}{3}\tau$, when the solution (100) exists for any ν .

III. PHASE

Consider the interaction of an atomic cloud with a sequence of three main resonant Raman pulses $\pi/2 - \pi - \pi/2$, acting at the moments $\{T_{1,0}, T_{2,0}, T_{3,0}\}$, having duration

$$d_{\zeta,m} \equiv \begin{cases} T_{\zeta,m} - T_{\zeta,m-1} - \tau(\nu, \zeta, m-1, \ell_{\zeta,m-1}) & \text{for } -2n < m \leq 2n \\ T \equiv T_{\zeta,-2n} - T_{\zeta-1,2n} - \tau(\nu, \zeta-1, 2n, \ell_{\zeta-1,2n}) & \text{for } m = -2n, \zeta > 1, \end{cases} \quad (110)$$

i.e., we define the interrogation time T as the time between the end of the last auxiliary NCP $\{1, 2n\}$ and the beginning of the first auxiliary NCP $\{2, -2n\}$, which coincides with the time between the end of the last auxiliary NCP $\{2, 2n\}$ and the beginning of the first auxiliary NCP $\{3, -2n\}$. From the given $T_{1,0}$, delays between NCPs (110) and their durations (106) and (109) one can make up the full timing, the moments of action of each of the pulses $T_{\zeta,\beta}$. One can represent them as

$$T_{\zeta,\beta} = T_{\zeta,\beta}^{(0)} + \Upsilon_{\zeta,\beta}, \quad (111)$$

where $T_{\zeta,\beta}^{(0)}$ is $T_{1,0}$ plus the sum of all preceding delays, while $\Upsilon_{\zeta,\beta}$ is the sum of the durations of all preceding pulses.

In this article, we neglect the deviations of pulses from the ideal shape and duration calculated below. Therefore, the gray lines on the recoil diagram associated with these deviations do not appear. We also assume negligible diagonal elements in s matrices (77), (85), and (96) and off-diagonal elements in s matrices (76a), (94a), and (105a). So the gray lines associated with the finite duration of the Raman pulses do not appear either. As a result, only two branches, blue and red, remain on the recoil diagram. In this case, the wave function of an atom is a column,

$$\underline{\chi} = \begin{pmatrix} \chi_b \\ \chi_r \end{pmatrix}. \quad (112)$$

After the action of the $\pi/2$ pulse $\{1, 0\}$ from Eqs. (61) and (107) one will find that this column is

$$\begin{pmatrix} c(e, \mathbf{p}_+^{(1,0)} + \hbar\mathbf{k}, T_{1,0} + \tau) \\ c(g, \mathbf{p}_+^{(1,0)}, T_{1,0} + \tau) \end{pmatrix} = \begin{pmatrix} S_{eg}^{(1,0)}(\mathbf{p}_+^{(1,0)} + \hbar\mathbf{k}/2) \\ S_{gg}^{(1,0)}(\mathbf{p}_+^{(1,0)} + \hbar\mathbf{k}/2) \end{pmatrix}, \quad (113)$$

$\tau - 2\tau - \tau$ and effective wave vector \mathbf{k} . Suppose that the atom was launched at $t = 0$ in the ground state, i.e., at $t < T_{1,0}$,

$$c(e, \mathbf{p}, t) = 0, \quad (107a)$$

$$c(g, \mathbf{p}, t) = \sqrt{f_g(\mathbf{p})}, \quad (107b)$$

where $f_g(\mathbf{p})$ is the momentum distribution function in the atomic cloud. Below, up to Eq. (136), to simplify the calculation, we omit the factor $\sqrt{f_g(\mathbf{p})}$. Regarding the auxiliary Raman π pulses, we will assume that there is an even number of them $2n$ in each of the four sets. All pulses, main and auxiliary, are numbered with integers $\{\zeta, \beta\}$, where $1 \leq \zeta \leq 3$. The numbers of the main pulses are $\{\zeta, 0\}$, and for the auxiliary NCPs at $\zeta = 1$ the values $1 \leq \beta \leq 2n$ correspond to the set following the first main $\pi/2$ pulse, at $\zeta = 2$ the values $-2n \leq \beta \leq -1$ and $1 \leq \beta \leq 2n$ correspond to the pulses that preceded or followed after the second main π pulse, and at $\zeta = 3$ the values $-2n \leq \beta \leq -1$ correspond to the set preceding the third main $\pi/2$ pulse. Each of the pulses is an NCP, consisting of $1 \leq \ell_{\zeta,\beta} \leq 3$ rectangular pulses. The effective wave vector and momentum chirp rate are

$$\mathbf{k}_{\zeta,\beta} = (-1)^\beta \mathbf{k}, \quad (108a)$$

$$\alpha_{\zeta,\beta} = (-1)^\beta \alpha \quad (108b)$$

and the total duration $\tau(\nu, \zeta, \beta, \ell_{\zeta,\beta})$ for auxiliary NCPs is given in Eqs. (106); for the main pulses there are

$$\tau(0, 1, 0, 1) = \tau(0, 2, 0, 1)/2 = \tau(0, 3, 0, 1) = \tau. \quad (109)$$

Here one takes into account that the main pulses are resonant for the blue and red branches of the recoil diagram, i.e., for them $\nu^{(0)} = 0$. In our calculations, we take into account the finite durations of the Raman pulses. For their timing, following Ref. [71], we introduce a delay time between pulses

where the matrix $S(\mathbf{P})$ is given in Eq. (62a). At resonance, when

$$v_r^{(0)} = \delta_{1,0}^{(0)}(\mathbf{p}_{+,T_{1,0}+\tau}^{(1,0)} + \hbar\mathbf{k}/2) = \delta_{1,0} - \frac{\mathbf{k}}{M} \cdot \mathbf{p}_{+,T_{1,0}+\tau}^{(1,0)} - \omega_k \approx 0 \quad (114)$$

and $|\Omega_{1,0}|$ given in Eq. (78), from Eqs. (56b), (46a), (46d), and (75a) it follows that

$$\underline{s} = \frac{1}{\sqrt{2}} \begin{pmatrix} 1 & -i \exp(i \arg \Omega_{1,0}) \\ -i \exp(i \arg \Omega_{1,0}) & 1 \end{pmatrix}, \quad (115a)$$

$$v_r^{(0)} = \delta_{1,0} - \frac{\mathbf{k}}{M} \cdot \mathbf{p}_{+,T_{1,0}+\tau}^{(1,0)} - \omega_k, \quad (115b)$$

$$v_r = -(\mathbf{k} \cdot \mathbf{g} - \alpha)T_{1,0}, \quad (115c)$$

$$\phi_{1,0}(\mathbf{p}_{+,T_{1,0}+\tau}^{(1,0)} + \hbar\mathbf{k}/2) = \phi_{1,0} + \left(\delta_{1,0} - \frac{\mathbf{k}}{M} \cdot \mathbf{p}_{+,T_{1,0}+\tau}^{(1,0)} - \omega_k \right) T_{1,0} - \frac{1}{2}(\mathbf{k} \cdot \mathbf{g} - \alpha)T_{1,0}^2, \quad (115d)$$

$$s'_d = \frac{i\sqrt{2}}{\pi}, \quad (115e)$$

respectively. Despite the resonance, we retained the Ramsey term [74] [the second term in the expression for the phase (115d)]. For resonance it is enough that

$$|v_r^{(0)}| \ll \tau^{-1}. \quad (116)$$

If

$$T_{1,0} \sim T \gg \tau, \quad (117)$$

then, despite the resonance condition, one can observe Ramsey fringes at

$$T^{-1} \lesssim |v_r^{(0)}| \ll \tau^{-1}. \quad (118)$$

From Eqs. (113), (62), and (115) one gets

$$\begin{pmatrix} c(e, \mathbf{p}_+^{(1,0)} + \hbar\mathbf{k}, T_{1,0} + \tau) \\ c(g, \mathbf{p}_+^{(1,0)}, T_{1,0} + \tau) \end{pmatrix} = \frac{1}{\sqrt{2}} \begin{pmatrix} \exp(i\psi_{1,0}^{(b)}) \\ \exp(i\psi_{1,0}^{(r)}) \end{pmatrix}, \quad (119a)$$

$$\psi_{1,0}^{(b)} = -\frac{\pi}{2} - \phi_{1,0} + \arg \Omega_{1,0} - \left(\delta_{1,0} - \frac{\mathbf{k}}{M} \cdot \mathbf{p}_{+,T_{1,0}+\tau}^{(1,0)} - \omega_k \right) T_{1,0} + \frac{1}{2}(\mathbf{k} \cdot \mathbf{g} - \alpha)T_{1,0}^2 + \frac{1}{2}(\mathbf{k} \cdot \mathbf{g} - \alpha)T_{1,0}\tau, \quad (119b)$$

$$\psi_{1,0}^{(r)} = \left(\frac{2}{\pi} - \frac{1}{2} \right) (\mathbf{k} \cdot \mathbf{g} - \alpha)T_{1,0}\tau. \quad (119c)$$

With the exception of the last beam splitter $\{3, 0\}$, all subsequent beam splitters are π pulses. An ideal π pulse does not change the magnitude of states; only the phases of these states change. These changes, phase augmentations, in sum determine the phase of the interferometer.

Let us now consider the action of an odd NCP $\{1, 2m - 1\}$, for which $\mathbf{k}_{1,2m-1} = -\mathbf{k}$. Before interaction

$$\underline{\chi} = \begin{pmatrix} c(e, \pi_-, T_{1,2m-1}) \\ c(g, \mathbf{p}_-^{(1,2m-1)}, T_{1,2m-1}) \end{pmatrix} = \frac{1}{\sqrt{2}} \begin{pmatrix} \exp(i\psi_{1,2m-2}^{(b)}) \\ \exp(i\psi_{1,2m-2}^{(r)}) \end{pmatrix}. \quad (120)$$

From the recoil diagrams in Figs. 2 and 3 one can conclude that on the resonant branch, for arbitrary m , the preceding Raman pulses transferred to the atom an odd number of momenta $\hbar\mathbf{k}$, i.e.,

$$\pi_- = \mathbf{p}_-^{(1,2m-1)} + (2m - 1)\hbar\mathbf{k}. \quad (121)$$

Then, along the blue resonance branch after the NCP, from Eqs. (64b) and (108a) for $\mathfrak{N} = 2m$ the state of the atom changes as

$$c(g, \pi_+, T_{1,2m-1} + \tau_p) = S_{ge}^{(1,2m-1)}(\pi_s)c(e, \pi_-, T_{1,2m-1}), \quad (122a)$$

$$\pi_+ = \mathbf{p}_+^{(1,2m-1)} + 2m\hbar\mathbf{k}, \quad (122b)$$

$$\tau_p = \tau(v, 1, 2m - 1, \ell_{1,2m-1}), \quad (122c)$$

$$\pi_s = \pi + (4m - 1)\hbar\mathbf{k}/2, \quad (122d)$$

$$\pi = \mathbf{p}_{+,T_{1,2m-1}+\tau_p}^{(1,2m-1)}. \quad (122e)$$

In this case, under the condition of resonance

$$v_r^{(0)} = \delta_{1,2m-1}^{(0)}(\pi_s) = \left\{ \delta_{1,2m-1} + \frac{\mathbf{k}}{M} \cdot \pi \right\} + (4m-1)\omega_k \approx 0, \quad (123a)$$

$$v_r = (\mathbf{k} \cdot \mathbf{g} - \alpha)T_{1,2m-1}, \quad (123b)$$

$$\phi_{1,2m-1}(\pi_s) = \phi_{1,2m-1} + \left(\delta_{1,2m-1} + \frac{\mathbf{k}}{M} \cdot \pi + (4m-1)\omega_k \right) T_{1,2m-1} + \frac{1}{2}(\mathbf{k} \cdot \mathbf{g} - \alpha)T_{1,2m-1}^2, \quad (123c)$$

and then, using the off-diagonal matrix element in the s matrices (77), (83), and (96), from Eqs. (122), (62), and (123) one obtains

$$c(g, \pi_+, T_{1,2m-1} + \tau_p) = \frac{1}{\sqrt{2}} \exp(i\psi_{1,2m-1}^{(b)}), \quad (124a)$$

$$\psi_{1,2m-1}^{(b)} = \psi_{1,2m-2}^{(b)} + A_{1,2m-1}^{(b)}, \quad (124b)$$

$$A_{1,2m-1}^{(b)} = -\frac{\pi}{2} + \phi_{1,2m-1} - \arg \Omega_{1,2m-1} + \left(\delta_{1,2m-1} + \frac{\mathbf{k}}{M} \cdot \pi + (4m-1)\omega_k \right) T_{1,2m-1}^{(0)} + \frac{1}{2}(\mathbf{k} \cdot \mathbf{g} - \alpha)T_{1,2m-1}^2 + \frac{1}{2}(\mathbf{k} \cdot \mathbf{g} - \alpha)T_{1,2m-1}^{(0)}\tau_p, \quad (124c)$$

where $A_{1,2m-1}^{(b)}$ is the phase augmentation of the atomic amplitude on the blue branch during interaction with the NCP $\{1, 2m-1\}$. In the expression (124c) we have replaced

$$T_{\zeta,\beta} \rightarrow T_{\zeta,\beta}^{(0)} \quad (125)$$

in the fourth and last terms. This is because in the resonance condition (116)

$$|v_r| \Upsilon_{\zeta,\beta} \ll 1. \quad (126)$$

We also took into account that one can neglect the term $\Upsilon_{\zeta,\beta}\tau$ since it is bilinear in pulse durations.

Consider now the nonresonant red branch, where

$$c(g, \mathbf{p}_+^{(1,2m-1)}, T_{1,2m-1} + \tau_p) = S_{gg}^{(1,2m-1)}(\pi - \hbar\mathbf{k}/2)c(g, \mathbf{p}_-^{(1,2m-1)}, T_{1,2m-1}). \quad (127)$$

From Eqs. (46) and (123a) one finds

$$v = \delta_{1,2m-1}(\pi - \hbar\mathbf{k}/2) = \left\{ \delta_{1,2m-1} + \frac{\mathbf{k}}{M} \cdot \pi \right\} - \omega_k + (\mathbf{k} \cdot \mathbf{g} - \alpha)T_{1,2m-1}. \quad (128)$$

Since the terms in curly brackets in Eqs. (123a) and (128) coincide, then

$$v = -4m\omega_k + (\mathbf{k} \cdot \mathbf{g} - \alpha)T_{1,2m-1}. \quad (129)$$

Thus, knowing that there is no frequency detuning on the resonant branch of the recoil diagram, one is able to determine the detuning ν on the nonresonant branch. Since at a negligibly small recoil frequency there is no detuning on both branches, then at $\omega_k \neq 0$ the detuning ν is determined only by the recoil frequency and the Doppler frequency shift does not contribute to it.

The second term in Eq. (129) is a small correction associated with the finite duration of the NCP. One sees that in order to fulfill requirement (ii), the total duration of the NCP must be equal to

$$\tau_p = \tau(-4m\omega_k, 1, 2m-1, \ell_{1,2m-1}) \quad (130)$$

given by Eqs. (106). Then using the matrix element s_{gg} in s matrices (76a), (94a), and (105a), from Eqs. (127), (62), and (129) one finds that

$$c(g, \mathbf{p}_+^{(1,2m-1)}, T_{1,2m-1} + \tau_p) = \frac{1}{\sqrt{2}} \exp(i\psi_{1,2m-1}^{(r)}), \quad (131a)$$

$$\psi_{1,2m-1}^{(r)} = \psi_{1,2m-2}^{(r)} + A_{1,2m-1}^{(r)}, \quad (131b)$$

$$A_{1,2m-1}^{(r)} = -2m\omega_k\tau_p + \eta_0^{(\ell_{1,2m-1})} + \eta_0^{(\ell_{1,2m-1})}(-4m\omega_k) + \left[\frac{1}{2}\tau_p + \eta_1^{(\ell_{1,2m-1})}(-4m\omega_k) \right] (\mathbf{k} \cdot \mathbf{g} - \alpha)T_{1,2m-1}^{(0)}, \quad (131c)$$

where $\eta_0^{(\ell_{1,2m-1})}$ is given by Eqs. (76b), (91b), and (102b);

$$\eta_0^{(1)}(\nu) = 0; \quad (132)$$

$\eta_0^{(2)}(\nu)$ and $\eta_0^{(3\pm)}(\nu)$ are given by Eqs. (91c) and (102c), respectively; and $\eta_1^{(\ell)}(\nu)$ are given by Eqs. (76c), (94b), and (105b). In the last term, we also made a replacement (125).

The action of the remaining π pulses can be calculated in a similar way. One can verify that the ideal π pulse $\{\zeta, \beta\}$, for which one assigns the duration exactly according to the expressions (106) and which is in resonance with atomic transitions with an accuracy much lower than the inverse pulse duration, leads only to phase augmentation of the atomic state amplitudes $A_{\zeta, \beta}^{(b,r)}$. One arrives at the expressions for these augmentations

$$A_{1,m}^{(b)} = -\frac{\pi}{2} - (-1)^m(\phi_{1,m} - \arg \Omega_{1,m}) - \left((-1)^m \delta_{1,m} - \frac{\mathbf{k}}{M} \cdot \pi - (2m+1)\omega_k \right) T_{1,m}^{(0)} + \frac{1}{2}(\mathbf{k} \cdot \mathbf{g} - \alpha) T_{1,m}^2 + \frac{1}{2}(\mathbf{k} \cdot \mathbf{g} - \alpha) T_{1,m}^{(0)} \tau_p, \quad (133a)$$

$$A_{1,m}^{(r)} = (-1)^m \xi_m \omega_k \tau_p + \eta_0^{(\ell_{1,m})} + \eta_0^{(\ell_{1,m})} [(-1)^m 2\xi_m \omega_k] - (-1)^m \left\{ \frac{1}{2} \tau_p + \eta_1^{(\ell_{1,m})} [(-1)^m 2\xi_m \omega_k] \right\} (\mathbf{k} \cdot \mathbf{g} - \alpha) T_{1,m}^{(0)}, \quad (133b)$$

$$A_{2,-m}^{(b)} = -\frac{\pi}{2} + (-1)^m(\phi_{2,-m} - \arg \Omega_{2,-m}) + \left((-1)^m \delta_{2,-m} - \frac{\mathbf{k}}{M} \cdot \pi - (2m+1)\omega_k \right) T_{2,-m}^{(0)} - \frac{1}{2}(\mathbf{k} \cdot \mathbf{g} - \alpha) T_{2,-m}^2 - \frac{1}{2}(\mathbf{k} \cdot \mathbf{g} - \alpha) T_{2,-m}^{(0)} \tau_p, \quad (133c)$$

$$A_{2,-m}^{(r)} = (-1)^m \xi_m \omega_k \tau_p + \eta_0^{(\ell_{2,-m})} + \eta_0^{(\ell_{2,-m})} [(-1)^m 2\xi_m \omega_k] - (-1)^m \left\{ \frac{1}{2} \tau_p + \eta_1^{(\ell_{2,-m})} [(-1)^m 2\xi_m \omega_k] \right\} (\mathbf{k} \cdot \mathbf{g} - \alpha) T_{2,-m}^{(0)}, \quad (133d)$$

$$A_{2,0}^{(b)} = -\frac{\pi}{2} + \phi_{2,0} - \arg \Omega_{2,0} + \left(\delta_{2,0} - \frac{\mathbf{k}}{M} \cdot \mathbf{p}_{+, T_{2,0}+2\tau}^{(2,0)} - \omega_k \right) T_{2,0}^{(0)} - \frac{1}{2}(\mathbf{k} \cdot \mathbf{g} - \alpha) T_{2,0}^2 - (\mathbf{k} \cdot \mathbf{g} - \alpha) T_{2,0}^{(0)} \tau, \quad (133e)$$

$$A_{2,0}^{(r)} = -\pi - A_{2,0}^{(b)}, \quad (133f)$$

$$A_{2,m}^{(b)} = (-1)^m \xi_m \omega_k \tau_p + \eta_0^{(\ell_{2,m})} + \eta_0^{(\ell_{2,m})} [(-1)^m 2\xi_m \omega_k] - (-1)^m \left\{ \frac{1}{2} \tau_p + \eta_1^{(\ell_{2,m})} [(-1)^m 2\xi_m \omega_k] \right\} (\mathbf{k} \cdot \mathbf{g} - \alpha) T_{2,m}^{(0)}, \quad (133g)$$

$$A_{2,m}^{(r)} = -\frac{\pi}{2} - (-1)^m(\phi_{2,m} - \arg \Omega_{2,m}) - \left((-1)^m \delta_{2,m} - \frac{\mathbf{k}}{M} \cdot \pi - (2m+1)\omega_k \right) T_{2,m}^{(0)} + \frac{1}{2}(\mathbf{k} \cdot \mathbf{g} - \alpha) T_{2,m}^2 + \frac{1}{2}(\mathbf{k} \cdot \mathbf{g} - \alpha) T_{2,m}^{(0)} \tau_p, \quad (133h)$$

$$A_{3,-m}^{(b)} = (-1)^m \xi_m \omega_k \tau_p + \eta_0^{(\ell_{3,-m})} + \eta_0^{(\ell_{3,-m})} [(-1)^m 2\xi_m \omega_k] - (-1)^m \left\{ \frac{1}{2} \tau_p + \eta_1^{(\ell_{3,-m})} [(-1)^m 2\xi_m \omega_k] \right\} (\mathbf{k} \cdot \mathbf{g} - \alpha) T_{3,-m}^{(0)}, \quad (133i)$$

$$A_{3,-m}^{(r)} = -\frac{\pi}{2} + (-1)^m(\phi_{3,-m} - \arg \Omega_{3,-m}) + \left((-1)^m \delta_{3,-m} - \frac{\mathbf{k}}{M} \cdot \pi - (2m+1)\omega_k \right) T_{3,-m}^{(0)} - \frac{1}{2}(\mathbf{k} \cdot \mathbf{g} - \alpha) T_{3,-m}^2 - \frac{1}{2}(\mathbf{k} \cdot \mathbf{g} - \alpha) T_{3,-m}^{(0)} \tau_p, \quad (133j)$$

where

$$\xi_m = m + \frac{1}{2}[1 - (-1)^m]. \quad (134)$$

In the expressions for augmentations $A_{\zeta, \beta}^{(b,r)}$ the duration of the pulse $\{\zeta, \beta\}$, τ_p , and momentum π are given by

$$\tau_p = \tau [(-1)^\beta 2\xi_\beta \omega_k, \zeta, \beta, \ell_{\zeta, \beta}], \quad (135a)$$

$$\pi = \mathbf{p}_{+, T_{\zeta, \beta} + \tau_p}^{(\zeta, \beta)}. \quad (135b)$$

The augmentations (133a), (133c), (133e), (133f), (133h), and (133j) refer to the resonant branch of the recoil diagram, while the augmentations (133b), (133d), (133g), and (133i) refer to the nonresonant branch.

The factor $(-1)^m$ reflects the fact that at the transitions $g \rightarrow e$ and $e \rightarrow g$ one uses different off-diagonal elements of the matrix S in Eq. (62) and for them the signs of the phase factors are opposite. As a result, the terms associated with the detuning δ change sign. However, at the same time, the terms associated with the Doppler shift and the gravitational field remain unchanged, because for transitions $g \rightarrow e$ and $e \rightarrow g$ one uses opposite effective wave vectors $\pm \mathbf{k}$.

Using the augmentations (133), one calculates the phases of the atomic state amplitudes before the action of the third main $\pi/2$ pulse $\{\psi_{3,-1}^{(b)}, \psi_{3,-1}^{(r)}\}$. We are interested in the total probability of excitation of atoms in the cloud

$$w = \int d\mathbf{p}_+^{(3,0)} f_g(\mathbf{p}_+^{(3,0)}) |c(e, \mathbf{p}_+^{(3,0)} + \hbar \mathbf{k}, T_{3,0} + \tau)|^2, \quad (136)$$

where we have restored the factor $\sqrt{f_g(\mathbf{p})}$ from Eq. (107b). At $t = T_{3,0} + \tau$ the amplitude of an atom in an excited state consists of blue and red components,

$$c(e, \mathbf{p}_+^{(3,0)} + \hbar\mathbf{k}, T_{3,0} + \tau) = c^{(b)}(e, \mathbf{p}_+^{(3,0)} + \hbar\mathbf{k}, T_{3,0} + \tau) + c^{(r)}(e, \mathbf{p}_+^{(3,0)} + \hbar\mathbf{k}, T_{3,0} + \tau), \quad (137)$$

for which one has

$$c^{(b)}(e, \mathbf{p}_+^{(3,0)} + \hbar\mathbf{k}, T_{3,0} + \tau) = S_{eg}^{(3,0)}(\mathbf{p}_{+,T_{3,0}+\tau}^{(3,0)} + \hbar\mathbf{k}/2)c(g, \mathbf{p}_-^{(3,0)}, T_{3,0}), \quad (138a)$$

$$c^{(r)}(e, \mathbf{p}_+^{(3,0)} + \hbar\mathbf{k}, T_{3,0} + \tau) = S_{ee}^{(3,0)}(\mathbf{p}_{+,T_{3,0}+\tau}^{(3,0)} + \hbar\mathbf{k}/2)c(e, \mathbf{p}_-^{(3,0)} + \hbar\mathbf{k}, T_{3,0}). \quad (138b)$$

After calculations similar to those used in the derivation of Eqs. (119), one obtains

$$\begin{pmatrix} c^{(b)}(e, \mathbf{p}_+^{(3,0)} + \hbar\mathbf{k}, T_{3,0} + \tau) \\ c^{(r)}(e, \mathbf{p}_+^{(3,0)} + \hbar\mathbf{k}, T_{3,0} + \tau) \end{pmatrix} = \frac{1}{2} \begin{pmatrix} \exp(i\psi_{3,0}^{(b)}) \\ \exp(i\psi_{3,0}^{(r)}) \end{pmatrix}, \quad (139a)$$

$$\psi_{3,0}^{(b,r)} = \psi_{3,-1}^{(b,r)} + A_{3,0}^{(b,r)}, \quad (139b)$$

$$\begin{aligned} A_{3,0}^{(b)} = & -\frac{\pi}{2} - \phi_{3,0} + \arg \Omega_{3,0} - \left(\delta_{3,0} - \frac{\mathbf{k}}{M} \cdot \mathbf{p}_{+,T_{3,0}+\tau}^{(3,0)} - \omega_k \right) T_{3,0}^{(0)} \\ & + \frac{1}{2}(\mathbf{k} \cdot \mathbf{g} - \alpha)T_{3,0}^2 + \frac{1}{2}(\mathbf{k} \cdot \mathbf{g} - \alpha)T_{3,0}\tau, \end{aligned} \quad (139c)$$

$$A_{3,0}^{(r)} = \left(\frac{1}{2} - \frac{2}{\pi} \right) (\mathbf{k} \cdot \mathbf{g} - \alpha) T_{3,0}^{(0)} \tau. \quad (139d)$$

In Eq. (137) the independent variable is the momentum of the atom after the action of the pulse $\{3, 0\}$, $\mathbf{p}_+^{(3,0)}$. Using Eqs. (65) and (66b), one can calculate the values of all other momenta in Eqs. (133). Such calculations would be necessary if we were only interested in one of the ports in Figs. 1–3. The total excitation probability (136) is the sum of the probabilities over all possible ports. For this response, in Eq. (136) one introduces a new integration variable

$$\mathbf{p}_i = \mathbf{p}_{+,T_{3,0}+\tau}^{(3,0)}. \quad (140)$$

From Eq. (60b) it follows that all pulses in Eqs. (133) coincide with \mathbf{p}_i .

This coincidence is a consequence of the fact that in Eq. (63) one selected in the momentum the parts associated with the transfer of photon momenta $\mathcal{N}\hbar\mathbf{k}$ and the momentum that changes only under the action of the gravitational field.

The integrand in Eq. (136) is a rapidly oscillating function momentum \mathbf{p}_i with a period of the order of M/kT . One chooses the timing of the pulses in the AI such that these oscillations disappear. If, in addition, the atomic cloud is cooled to such a temperature that the momentum in the functions of the parameters s_d and s_a from Eqs. (56) can be considered to be the same as the average momentum in the cloud, then one will receive

$$w = \frac{1}{2}(1 - \cos \phi), \quad (141)$$

where the phase of the atomic interferometer is

$$\phi = \pi + \psi_{3,0}^{(b)} - \psi_{3,0}^{(r)} = \pi + \sum_{j=1}^3 A_{j,0} + \sum_{m=1}^{2n} (A_{1,m} + A_{2,-m} + A_{2,m} + A_{3,-m}), \quad (142a)$$

$$A_{\zeta,\beta} \equiv \begin{cases} \psi_{1,0}^{(b)} - \psi_{1,0}^{(r)} & \text{for } \{\zeta, \beta\} = \{1, 0\} \\ A_{\zeta,\beta}^{(b)} - A_{\zeta,\beta}^{(r)} & \text{for } \{\zeta, \beta\} \neq \{1, 0\}. \end{cases} \quad (142b)$$

Then from Eqs. (119b), (119c), (133), (139c), and (139d) one arrives at the next result

$$\phi = \bar{\phi} + \phi_R + \phi_D + \phi_q + \bar{\phi}_q + \phi_g^{(0)} + \phi_g^{(1)}, \quad (143)$$

where

$$\bar{\phi} = -\phi_{1,0} + 2\phi_{2,0} - \phi_{3,0} - \sum_{m=1}^{2n} \{ (-1)^m [\phi_{1,m} - \phi_{2,-m} - \phi_{2,m} + \phi_{3,-m}] + \eta_0^{(\ell_{1,m})} + \eta_0^{(\ell_{2,-m})} - \eta_0^{(\ell_{2,m})} - \eta_0^{(\ell_{3,-m})} \}, \quad (144)$$

the Ramsey phase

$$\phi_R = -\delta_{1,0}T_{1,0} + 2\delta_{2,0}T_{2,0}^{(0)} - \delta_{3,0}T_{3,0}^{(0)} + \sum_{m=1}^{2n} (-1)^m (-\delta_{1,m}T_{1,m}^{(0)} + \delta_{2,-m}T_{2,-m}^{(0)} + \delta_{2,m}T_{2,m}^{(0)} - \delta_{3,-m}T_{3,-m}^{(0)}), \quad (145)$$

the Doppler phase

$$\phi_D = \frac{\mathbf{k}}{M} \cdot \mathbf{p}_i \left(T_{1,0} - 2T_{2,0}^{(0)} + T_{3,0}^{(0)} + \sum_{m=1}^{2n} (T_{1,m}^{(0)} - T_{2,-m}^{(0)} - T_{2,m}^{(0)} + T_{3,-m}^{(0)}) \right), \quad (146)$$

the quantum phases

$$\phi_q = \omega_k \left(T_{1,0} - 2T_{2,0}^{(0)} + T_{3,0}^{(0)} + \sum_{m=1}^{2n} (2m+1)(T_{1,m}^{(0)} - T_{2,-m}^{(0)} - T_{2,m}^{(0)} + T_{3,-m}^{(0)}) \right), \quad (147a)$$

$$\begin{aligned} \bar{\phi}_q = \sum_{m=1}^{2n} \{ & -\eta_0^{(\ell_{1,m})} [(-1)^m 2\xi_m \omega_k] - \eta_0^{(\ell_{2,-m})} [(-1)^m 2\xi_m \omega_k] + \eta_0^{(\ell_{2,m})} [2(-1)^m \xi_m \omega_k] \\ & + \eta_0^{(\ell_{3,-m})} [(-1)^m 2\xi_m \omega_k] + (-1)^m \xi_m \omega_k [-\tau((-1)^m 2\xi_m \omega_k, 1, m, \ell_{1,m}) - \tau((-1)^m 2\xi_m \omega_k, 2, -m, \ell_{2,-m}) \\ & + \tau((-1)^m 2\xi_m \omega_k, 2, m, \ell_{2,m}) + \tau((-1)^m 2\xi_m \omega_k, 3, -m, \ell_{3,-m})] \}, \end{aligned} \quad (147b)$$

the gravity phases

$$\phi_g^{(0)} = \frac{1}{2} (\mathbf{k} \cdot \mathbf{g} - \alpha) \left(T_{1,0}^{(0)2} - 2T_{2,0}^{(0)2} + T_{3,0}^{(0)2} + \sum_{m=1}^{2n} (T_{1,m}^{(0)2} - T_{2,-m}^{(0)2} - T_{2,m}^{(0)2} + T_{3,-m}^{(0)2}) \right), \quad (148a)$$

$$\begin{aligned} \phi_g^{(1)} = (\mathbf{k} \cdot \mathbf{g} - \alpha) \left\{ & T_{1,0}^{(0)} \Upsilon_{1,0} - 2T_{2,0}^{(0)} \Upsilon_{2,0} + T_{3,0}^{(0)} \Upsilon_{3,0} + \tau \left[\left(1 - \frac{2}{\pi} \right) T_{1,0}^{(0)} - 2T_{2,0}^{(0)} + \frac{2}{\pi} T_{3,0}^{(0)} \right] \right. \\ & + \sum_{m=1}^{2n} [T_{1,m}^{(0)} \Upsilon_{1,m} - T_{2,-m}^{(0)} \Upsilon_{2,-m} - T_{2,m}^{(0)} \Upsilon_{2,m} + T_{3,-m}^{(0)} \Upsilon_{3,-m} \\ & + \{\zeta_{m+1} \tau((-1)^m 2\xi_m \omega_k, 1, m, \ell_{1,m}) + (-1)^m \eta_1^{(\ell_{1,m})} [(-1)^m 2\xi_m \omega_k] T_{1,m}^{(0)} \\ & - (\zeta_m \tau((-1)^m 2\xi_m \omega_k, 2, -m, \ell_{2,-m}) - (-1)^m \eta_1^{(\ell_{2,-m})} [(-1)^m 2\xi_m \omega_k] T_{2,-m}^{(0)} \\ & - \{\zeta_{m+1} \tau((-1)^m 2\xi_m \omega_k, 2, m, \ell_{2,m}) + (-1)^m \eta_1^{(\ell_{2,m})} [2(-1)^m \xi_m \omega_k] T_{2,m}^{(0)} \\ & \left. + \{\zeta_m \tau((-1)^m 2\xi_m \omega_k, 3, -m, \ell_{3,-m}) - (-1)^m \eta_1^{(\ell_{3,-m})} [2(-1)^m \xi_m \omega_k] T_{3,-m}^{(0)} \} \right\}, \end{aligned} \quad (148b)$$

and the parameter

$$\zeta_m \equiv \frac{1}{2} [1 - (-1)^m]. \quad (149)$$

IV. DOPPLER AND QUANTUM PHASES

The ultimate requirement for the MZAI is the zeroing of the Doppler phase (146), i.e., timing must be chosen in such a way that

$$\phi_D = 0. \quad (150)$$

Otherwise, the interference term in the excitation probability will be washed out when averaged over the momenta. In the absence of NCPs ($n = 0$), one will satisfy Eq. (150) if $T_{1,0} - 2T_{2,0}^{(0)} + T_{3,0}^{(0)} = 0$; however, then the quantum phase (147a) is also zeroed. The situation changes in the presence of NCPs. From Eq. (110) one can express the pulses' timing through the delays $T_{1,0}$ and T and delays between NCPs $d_{\zeta,\beta}$ as

$$T_{2,0}^{(0)} = T_{1,0} + T + \sum_{m=1}^{2n} (d_{1,m} + d_{2,-m+1}), \quad (151a)$$

$$T_{3,0}^{(0)} = T_{2,0}^{(0)} + T + \sum_{m=1}^{2n} (d_{2,m} + d_{3,-m+1}), \quad (151b)$$

$$T_{\zeta,m}^{(0)} = T_{\zeta,0}^{(0)} + \sum_{m'=1}^m d_{\zeta,m'}, \quad (151c)$$

$$T_{\zeta,-m}^{(0)} = T_{\zeta,0}^{(0)} - \sum_{m'=1}^m d_{\zeta,-m'+1}, \quad (151d)$$

where $m > 0$. From these equations one can find that the Doppler phase and the quantum phase are given by

$$\phi_D = \frac{\mathbf{k}}{M} \cdot \mathbf{p}_i \sum_{m=1}^{2n} m f_m, \quad (152a)$$

$$\phi_q = \omega_k \sum_{m=1}^{2n} m^2 f_m, \quad (152b)$$

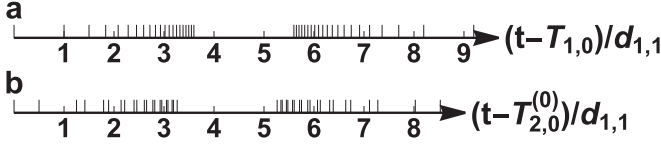


FIG. 6. Proposal for observing the quantum phase timing of the NCPs between the (a) first and second and (b) second and third main pulses at $n = 20$, $\varepsilon = 1/2$, and $T = 2d_{1,1}$.

where

$$f_m \equiv -d_{1,m} - d_{2,-m+1} + d_{2,m} + d_{3,-m+1}. \quad (153)$$

It is obvious that for $f_m \neq 0$, one can arrange the NCPs in such a way that the Doppler phase will be equal to 0 and atomic interference will occur, but the quantum phase will not disappear. We have calculated and offer the following possibility. Assume that the NCPs in the second and fourth sets are mirror images of the NCPs in the first and third sets,

$$d_{2,-m+1} = d_{1,m}, \quad (154a)$$

$$d_{3,-m+1} = d_{2,m}. \quad (154b)$$

The Doppler phase will be guaranteed to be zeroed if

$$f_m = \frac{(-1)^m}{m} f. \quad (155)$$

If, moreover, it is required that

$$d_{2,m} = [1 + (-1)^m \varepsilon] d_{1,m}, \quad (156)$$

then from Eqs. (153)–(155) for intervals between NCPs one gets

$$d_{1,m} = \frac{d_{1,1}}{m}. \quad (157)$$

The timing of NCPs spaced at intervals (156) and (157) is shown in Fig. 6 for $\varepsilon = \frac{1}{2}$.

Here one arrives at the expression for the quantum phase

$$\phi_q = \varepsilon \omega_k (T_{1,2n}^{(0)} - T_{1,0}) \frac{2n}{\psi(2n+1) + \gamma}, \quad (158)$$

where $\psi(z)$ is the digamma Euler function and γ is the Euler constant. For large n , the quantum phase grows as

$$\phi_q = \varepsilon \omega_k (T_{1,2n}^{(0)} - T_{1,0}) \frac{2n}{\ln 2n + \gamma}. \quad (159)$$

The quantum phase is shown in Fig. 7.

Phase $\bar{\phi}_q$

If the recoil frequency is comparable to the inverse pulse duration, then a smooth quantum phase dependence appears not on the distance between the pulses, but on the pulse duration. It arises owing to the fact that the amplitude of the atom in the ground state $|g\rangle$ on the nonresonant branch of the recoil diagram changes its phase, remaining unchanged in absolute value. The changes are due to the fact that the diagonal elements of the s matrices (76a), (94a), and (105a) contain phase factors and also to the fact that the pulse duration depends on the Raman detuning on the nonresonant branch [see Eq. (106)], which, according to Eq. (129), is

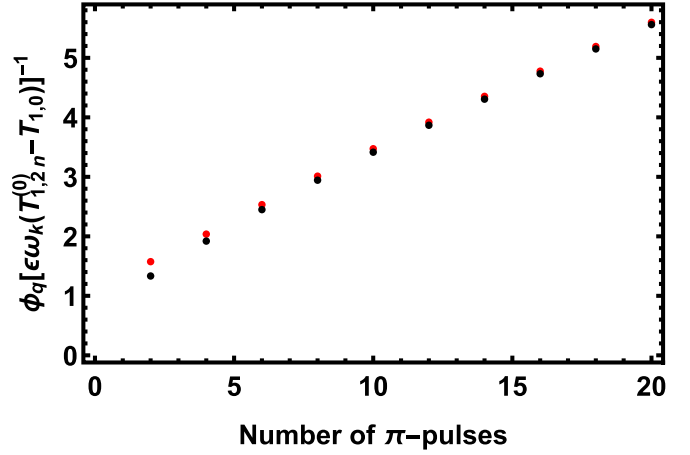


FIG. 7. Quantum phase as a function of the number of NCPs. Exact (158) and asymptotic (159) dependences are plotted in black and red, respectively.

determined by the recoil frequency. In the case of rectangular pulses, we calculated these changes [see phase augmentation in Eqs. (133b), (133d), (133g), and (133i)].

If all NCPs belong to the same class, $\ell_{\zeta,\beta} = \text{const}$, then from Eqs. (91c), (102c), (132), (106), and (147b) one could make sure that the phase $\bar{\phi}_q$ does not depend on recoil frequency,

$$\begin{aligned} \bar{\phi}_q|_{\ell_{\zeta,\beta}=1} = & \frac{\pi}{2} \sum_{m=1}^{2n} (-1)^m \left(-\sqrt{4j_{1,m,1}^2 - 1} - \sqrt{4j_{2,-m,1}^2 - 1} \right. \\ & \left. + \sqrt{4j_{2,m,1}^2 - 1} + \sqrt{4j_{3,-m,1}^2 - 1} \right), \end{aligned} \quad (160a)$$

$$\begin{aligned} \bar{\phi}_q|_{\ell_{\zeta,\beta}=2} = & \pi \sum_{m=1}^{2n} (-1)^m \left(-j_{1,m,2} - j_{2,-m,2} \right. \\ & \left. + j_{2,m,2} + j_{3,-m,2} \right), \end{aligned} \quad (160b)$$

$$\bar{\phi}_q|_{\ell_{\zeta,\beta}=3_{\pm}} = 0. \quad (160c)$$

In these equations, we omitted terms that are multiples of 2π . To obtain a phase dependent on ω_k , it is necessary that at least one NCP differs from others in the number of rectangular

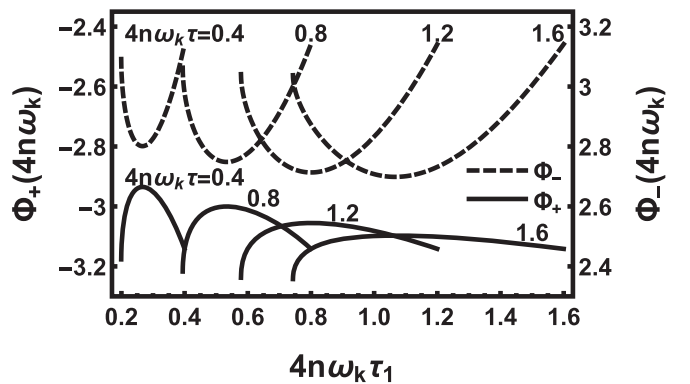


FIG. 8. Smooth dependence of the phase as a function of the duration of the first rectangular pulse in the NCP τ_1 for different values of the parameter $4n\omega_k\tau$.

pulses included in it. We have considered the case when for all NCPs $\ell_{\zeta,\beta} = 2$, except for the NCP $\{1.2n\}$, for which $\ell_{1.2n} = 3_{\pm}$. From Eqs. (90), (91c), (101b), (102c), and (147b) one arrives at the result

$$\bar{\phi}_q = \bar{\phi}_q|_{\ell_{\zeta,\beta}=2} + \frac{\pi}{2} + \Phi_{\pm}(4n\omega_k), \tag{161a}$$

$$\begin{aligned} \Phi_{\pm}(\nu) = & -2 \arctan \left[\frac{2\nu\tau}{\sqrt{\pi^2 + 4\nu^2\tau^2}} \tan \left(\frac{1}{4} \sqrt{\pi^2 + 4\nu^2\tau^2} \right) \right] + \arctan \left(\frac{2\nu\tau}{\sqrt{\pi^2 + 4\nu^2\tau^2}} \tan \frac{\tau_1}{4\tau} \sqrt{\pi^2 + 4\nu^2\tau^2} \right) \\ & + \arctan \frac{\text{Im}(s_{d1}s_{d2})}{\text{Re}(s_{d1}s_{d2})} \mp \left(\arccos \frac{1}{2} \left| \frac{s_{a2}}{s_{a1}s_{d1}} \right| + \arccos \frac{|s_{a2}|(|s_{a1}|^2 - |s_{d1}|^2)}{2|s_{a1}s_{d1}s_{d2}|} \right). \end{aligned} \tag{161b}$$

The dependences (161b) are shown in Fig. 8.

V. GRAVITY PHASE

The main reason for using SLMT is the increase in the gravitational phase of the AI. For this phase, from Eqs. (151) and (148a) one obtains

$$\begin{aligned} \phi_g^{(0)} = & (\mathbf{k} \cdot \mathbf{g} - \alpha) \left\{ (2n + 1)T^2 + T \sum_{m=1}^{2n} [(2n + 1 - m)d_{2,-m+1} + (2n + 1 + m)d_{2,m} + 2md_{3,-m+1}] \right. \\ & + \frac{2n + 1}{2} \left[\left(\sum_{m=1}^{2n} (d_{2,m} + d_{3,-m+1}) \right)^2 - \left(\sum_{m=1}^{2n} (d_{1,m} + d_{2,-m+1}) \right)^2 \right] \\ & + \frac{1}{2} \sum_{m=1}^{2n} \left[\left(\sum_{m'=1}^m d_{1,m'} \right)^2 - \left(\sum_{m'=1}^m d_{2,-m'+1} \right)^2 - \left(\sum_{m'=1}^m d_{2,m'} \right)^2 + \left(\sum_{m'=1}^m d_{3,-m'+1} \right)^2 \right] \\ & + \left(\sum_{m=1}^{2n} (d_{1,m} + d_{2,-m+1}) \right) \left(\sum_{m=1}^{2n} [(2n + 1 - m)d_{2,-m+1} + (2n + 1 + m)d_{2,m} + 2md_{3,-m+1}] \right) \\ & \left. - \left(\sum_{m=1}^{2n} (2n + 1 - m)d_{3,-m+1} \right) \left(\sum_{m=1}^{2n} (d_{2,m} + d_{3,-m+1}) \right) \right\}. \end{aligned} \tag{162}$$

Let us go to the calculation of the correction (148b). In the timing of a given Raman pulse (111), the $\Upsilon_{\zeta,\beta}$ part is the sum of the durations of all preceding pulses, i.e.,

$$\Upsilon_{\zeta,m} = \begin{cases} \sum_{m'=0}^{m-1} \tau(\nu, 1, m', \ell_{1,m'}) & \text{for } \zeta = 1 \\ \Upsilon_{\zeta-1,2n} + \tau(\nu, \zeta - 1, 2n, \ell_{\zeta-1,2n}) + \sum_{m'=-2n}^{m-1} \tau(\nu, \zeta, m', \ell_{\zeta,m'}) & \text{for } \zeta > 1. \end{cases} \tag{163}$$

Here it is convenient to pick out the durations of the main pulses (109) so that

$$\Upsilon_{1,m} = \tau + \Theta_{1,m}, \tag{164a}$$

$$\Upsilon_{2,m} = \begin{cases} \tau + \Theta_{2,m} & \text{for } -2n \leq m \leq 0 \\ 3\tau + \Theta_{2,m} & \text{for } 0 < m \leq 2n, \end{cases} \tag{164b}$$

$$\Upsilon_{3,m} = 3\tau + \Theta_{3,m}. \tag{164c}$$

Calculations bring one to the next result

$$\phi_g^{(1)} = \phi_{g\tau} + \phi_{ga}, \tag{165a}$$

$$\phi_{g\tau} = (\mathbf{k} \cdot \mathbf{g} - \alpha) \tau \left\{ T \left(4n + 2 + \frac{4}{\pi} \right) + 2 \sum_{m=1}^{2n} \left[\frac{1}{\pi} (d_{1,m} + d_{2,-m+1}) + \left(\frac{1}{\pi} + m \right) (d_{2,m} + d_{3,-m+1}) \right] \right\}, \tag{165b}$$

$$\begin{aligned} \phi_{ga} = & (\mathbf{k} \cdot \mathbf{g} - \alpha) \left\{ -2T_{2,0}^{(0)} \Theta_{2,0} + T_{3,0}^{(0)} \Theta_{3,0} + \sum_{m=1}^{2n} [(\Theta_{1,m} T_{1,m}^{(0)} - \Theta_{2,-m} T_{2,-m}^{(0)} - \Theta_{2,m} T_{2,m}^{(0)} + \Theta_{3,m} T_{3,-m}^{(0)}) \right. \\ & \left. + \{\zeta_{m+1} \tau ((-1)^m 2\xi_m \omega_k, 1, m, \ell_{1,m}) + (-1)^m \eta_1^{(\ell_{1,m})} [(-1)^m 2\xi_m \omega_k] \} T_{1,m}^{(0)} \right\} \end{aligned}$$

$$\begin{aligned}
 & + \left\{ \zeta_m \tau ((-1)^m 2\xi_m \omega_k, 2, -m, \ell_{2,-m}) - (-1)^m \eta_1^{(\ell_{2,-m})} [(-1)^m 2\xi_m \omega_k] \right\} T_{2,-m}^{(0)} \\
 & + \left\{ \zeta_{m+1} \tau ((-1)^m 2\xi_m \omega_k, 2, m, \ell_{2,m}) + (-1)^m \eta_1^{(\ell_{2,m})} [2(-1)^m \xi_m \omega_k] \right\} T_{2,m}^{(0)} \\
 & + \left\{ \zeta_m \tau ((-1)^m 2\xi_m \omega_k, 3, -m, \ell_{3,-m}) - (-1)^m \eta_1^{(\ell_{3,-m})} [2(-1)^m \xi_m \omega_k] \right\} T_{3,-m}^{(0)} \Big\}. \quad (165c)
 \end{aligned}$$

In the absence of auxiliary NCPs, at $n = 0$, one returns to the well-known result [72]

$$\phi_g = (\mathbf{k} \cdot \mathbf{g} - \alpha) \left[T^2 + \tau T \left(2 + \frac{4}{\pi} \right) \right]. \quad (166)$$

One should note that the correction (165a), as well as the gravitational phase (162), grows with the increase in the number of NCPs.

VI. DISCUSSION

The model adopted here, a rectangular pulse of the optical field, is widely used in atomic interferometry and in the theory of atomic clocks [75]. At the same time, we are not aware of the consideration of corrections related to the nonideal pulse shape. Such corrections arise due to the nonpermanent field amplitude inside the pulse and due to the nonzero duration of the forward and backward fronts of the pulse τ_f . So instead of one small parameter (1) in the Bragg regime, in our case at least two parameters should be small,

$$\delta|\Omega|/|\Omega| \ll 1, \quad (167a)$$

$$\omega_k \tau_f \ll 1, \quad (167b)$$

where $\delta|\Omega|$ is the deviation of the Rabi frequency from a constant value. The article [76] reported that the field intensity was kept constant with an accuracy of 1%, meaning that

$$\delta|\Omega|/|\Omega| \sim 5 \times 10^{-3} \quad (168)$$

can be implemented.

In Ref. [77] the front durations were 10 ns; with a typical value of $\omega_k \sim 10^5 \text{ s}^{-1}$ one has the estimate

$$\omega_k \tau_f \sim 10^{-3}. \quad (169)$$

The fact that the small parameters (167) are 40 or 200 times smaller than the parameter (1) allows us to hope that the SLMT option proposed here is feasible.

It should be noted that the durations of the fronts cannot decrease indefinitely, since for the applicability of the adiabatic elimination of the upper level amplitude in Eq. (27) the front duration must be long enough,

$$\Delta \tau_f \gg 1. \quad (170)$$

With a typical value of $\Delta \sim 2\pi \times 1 \text{ GHz}$, $\Delta \tau_f \sim 60$. If, however, one will be able to create pulses with picosecond fronts, then in order to use them in atomic interferometry, one must first increase the one-photon detuning Δ and, accordingly, the field intensity also needs to be increased.

We predict that the MZAI quantum phase will not disappear in our case. It arises due to the phase (46d) in the Schrödinger equation (45), which is also valid in both Bragg (1) and Raman-Nath (4) regimes. Nevertheless, the quantum

phase was not observed in either the Bragg regime in [30] or the Raman-Nath regime in [33]. One can explain it by the fact that in those articles the auxiliary pulses were timed out at equal distances and in this case the combination of delays between NCPs in Eq. (153) $f_m = 0$. If one places the NCPs nonequal distances, then our expression (152b) for the quantum phase ϕ_q can be directly used in the Bragg regime [30]. Here, for example, one can use the nonequidistant NCPs timing shown in Fig. 6.

Our result cannot be used in the Raman-Nath regime, since in this case the atomic momentum in the recoil diagram changes along both branches. An example of such a diagram is shown in [33]. In the Raman-Nath regime, the calculation of the quantum phase must be carried out again. We hope to carry out this calculation in the future.

If the time budget for auxiliary NCPs is comparable to the interrogation time T , then the quantum phase (158) at $n \sim \varepsilon \sim 1$ is comparable to the maximal expected quantum phase (19b). This is the fundamental difference between our case and the quantum phases considered in Refs. [60–64], where the quantum phases were only small additions.

Like the gravity phase (6b), the quantum phase grows with an increase in the number of auxiliary NCPs, i.e., with an increase in momentum transfer. However, since the momentum transfer occurs gradually, increasing by $\hbar \mathbf{k}$ under the action of each NCP, the quantum phase grows more slowly than the gravity one in the factor $\ln n$ [see Eq. (159)].

In this work, as in other papers, we assumed that the interrogation time T is the same between the first and second and between the second and third main Raman pulses. The SLMT technique allows us to make these times different, since the resulting Doppler phase can be compensated by Doppler phases during the operation of auxiliary NCPs. With such an opportunity, a quantum phase should also arise. We hope to consider this option in the future.

The quantum phase (158) is linear in time. This is not the only phase linear in time. Another linear phase observed by B. Young [78] is the Ramsey phase (145). In order to extract the quantum phase, we propose to scale all the delay times between pulses into a factor $1 + x$,

$$\{T_{1,0}, d_{\zeta,\beta}\} \rightarrow (1+x)\{T_{1,0}, d_{\zeta,\beta}\}. \quad (171)$$

If simultaneously one scales the Raman detunings as

$$\delta_{\zeta,\beta} \rightarrow \delta_{\zeta,\beta}/(1+x), \quad (172)$$

then the Ramsey phase (145) remains unchanged; only the quantum phase grows linearly in x , and the excitation probability w is a periodic function of x with period

$$\Delta x = 2\pi \left(\varepsilon \omega_k (T_{1,2n}^{(0)} - T_{1,0}) \frac{2n}{\psi(2n+1) + \gamma} \right)^{-1}. \quad (173)$$

To avoid violating the resonance condition (116) during scaling, the parameter x must be small,

$$x \ll (\omega_k \tau)^{-1}. \quad (174)$$

Since even for $n \sim 1$ and $\varepsilon \sim 1$,

$$\Delta x \omega_k \tau \sim \frac{\tau}{T_{1,2n}^{(0)} - T_{1,0}} \ll 1, \quad (175)$$

one can observe many periods of quantum oscillations of the excitation probability without significantly violating the resonance condition.

We predict a quantum effect, the dependence of the phase on the pulse durations τ and τ_1 , the term $\tilde{\phi}_q$. Unlike the phase linear in T (19b), the term $\tilde{\phi}_q$ is a nonlinear function of $\{\tau, \tau_1\}$. Another difference from the term (19b) is that it is specific only to the variant of SLMT considered here. Neither in the Bragg regime (1) nor in the Raman-Nath regime (4) does the term $\tilde{\phi}_q$ occur. Its appearance is due to the fact that the Raman frequency detuning on the nonresonant branch of the recoil diagram is proportional to the recoil frequency [see Eq. (129)]. This leads to the fact that in the case of NCPs of type $\ell = 1$, the pulse duration at which, owing to Rabi oscillations, the atom is not excited on the nonresonant branch also depends on ω_k [see Eqs. (73) and (129)]. If the NCPs type is $\ell > 1$, then the frequency detuning (129) is the atomic coherence nutation frequency in the space between pulses. Therefore, the delay between pulses τ_b also depends on ω_k [see Eqs. (90), (101b), and (129)]. Despite that the atoms remain in the ground state on the nonresonant branch of the recoil diagram, the phase of the amplitude of this state changes [see Eqs. (91) and (102)] and this change also contributes to the $\tilde{\phi}_q$ phase. If the rapidly oscillating quantum phase ϕ_q vanishes at an equidistant location of the NCPs, then the smooth phase $\tilde{\phi}_q$ also ceases to depend on the recoil frequency if all NCPs are of the same type [see Eqs. (160)]. It is necessary to use NCPs of different types. In Sec. IV we carried out the calculation in the case when all NCPs are of type $\ell = 2$, except for NCP $\{1, 2n\}$, whose type is $\ell_{1,2n} = 3$.

Another effect that disappears in the convenient MZAI but appears when additional beam splitters are turned on is the gravitational redshift [79].

Finally, the gravity phase (148a), being quadratic in the Raman pulses' timing, apart from the main term, the first term in curly brackets in Eq. (162), contains cross terms, combinations of interrogation time and delays $d_{\zeta,\beta}$, between auxiliary NCPs, and terms quadratic in $d_{\zeta,\beta}$. All these terms are pieced together in Eq. (162). From a mathematical point of view, the gravity phase is caused by the phase terms (46d) in the Schrödinger equation (45). Since this equation is valid for any pulse shape $f(t)$, our result (162) will also be correct in the Bragg regime, under the conditions of the experiment in [30].

The correction associated with the finite duration of the Raman pulse, on the contrary, depends on the pulse shape [80]. Therefore, the result (165) is only correct for rectangular NCPs.

In this work, we considered only MZAI. The SLMT method can lead to a significant increase in the AI phase in other cases as well, for the asymmetric MZAI [57], atomic two-loop gyroscopes [81], and gravity gradiometers [82]. Calculations of the SLMT technique for these AIs are left for

future work. As for the two-loop AIs, as shown in Ref. [61], the AI response occurs simultaneously with the stimulated echo response, the phase of which is sensitive to gravity acceleration. Two methods have been proposed to resolve this problem, the adjustable momentum transfer [61] and the time-skewed pulse sequence [83]. For atomic gyroscopes, both methods have been implemented in [83–86]. For the atomic gravity gradiometer, only the time-skewed method was used. However, even a small distortion in time led to the appearance of a significant background proportional to the gravity acceleration [82]. No background should occur in the adjustable momentum transfer method.

ACKNOWLEDGMENTS

I am grateful to M. Kasevich for discussing the work at an early stage, and to Brenton Young for bringing to me the observation of the Ramsey phase in his MZAI. I am also grateful to S. Kahn, A. Kumarakrishnan, V. I. Yudin, and A. V. Taichenashev for fruitful discussions.

APPENDIX: HIGHER-ORDER DENSITY HARMONICS

The atomic resonant Kapitza-Dirac effect [87] in the field of a standing wave and its analogs lie at the heart of many atomic beam splitters. The momentum transfer to an atom, which is a multiple of $\hbar k$, and the subsequent interference of atomic states with different momenta leads to the appearance of higher harmonics of the atomic density. Density harmonics with a period up to $\lambda/10$, where λ is the standing wavelength, have been observed in AIs [88]. Modifications of the standing wave, i.e., the triangular potential [89] and the bichromatic standing wave [90], have been proposed; moreover, transfer of momentum to an atom $\pm 21\hbar k$ was observed [89]. Despite the scattering of atoms at large angles, the scattering indicatrix contains not only the desired states $\pm n\hbar k$ but also neighboring states $\dots (\pm n - 2)\hbar k, (\pm n - 1)\hbar k, (\pm n + 1)\hbar k, (\pm n + 2)\hbar k \dots$. The asymptotes for $n \gg 1$ inner tails of this indicatrix were obtained in Refs. [91,92]. A complete indicatrix for three types of optical potentials was obtained in Ref. [93], where it was also shown that, due to neighboring momentum states, the interference pattern with a period of $\lambda/2n$ has a smooth envelope with a period of $\lambda/2$, and because of this, it is obvious that the possibility of using an AI of this type is doubtful, both for precision measurements and for nanolithography. To get rid of this difficulty, one can use [65] the Stern-Gerlach effect [94], i.e., an atom scattering in a magnetic field having a uniform gradient. It has been shown that one can obtain an atomic lattice with a period of 100 nm and a smooth envelope of size approximately equal to 100 μm , which arises owing to the weak inhomogeneity of the magnetic-field gradient. Another multicolor scheme was proposed in Ref. [95], where the beam splitter consisted of three traveling waves with frequencies and wave vectors $\{\Omega, \mathbf{k}\}$, $\{\Omega + \delta_1, -\mathbf{k}\}$, and $\{\Omega + \delta_2, -\mathbf{k}\}$. If the frequency detunings are chosen in such a way that $n_1\delta_1 + n_2\delta_2 = 0$, then this combination of fields creates an amplitude or phase diffraction grating for atoms with a period $\lambda/2(n_1 + n_2)$. If the standing wave is replaced by two counterpropagating waves in the lin \perp lin configuration, then such a field will be a diffraction phase grating for

atoms with a period of $\lambda/4$ [96,97]. Note also that the Raman standing-wave method was proposed [47]. This technique is now widely known as the double-diffraction scheme [48]. The main point of the method is that two Raman pulses with opposite effective wave vectors $\pm\mathbf{k}$ lead to splitting of the initial momentum state $|g, \mathbf{p}\rangle$ into two states $|e, \mathbf{p} \pm \hbar\mathbf{k}\rangle$. Since $k \approx 4\pi/\lambda$, then the interference between the scattered states leads to density modulation, the atomic lattice with a period

$\lambda/4$. If one of the Raman pulses has the configuration $\text{lin} \parallel \text{lin}$ and the configuration of the other is $\text{lin} \perp \text{lin}$, then the Raman standing wave induces an atomic lattice with a period $\lambda/8$ [47]. Scattering potentials with period $\lambda/8$ were calculated for various components of the hyperfine splitting of ^{85}Rb [98]. One can expect that the Raman standing-wave method, in combination with the multicolor technique, produces density harmonics with a period $\lambda/8n$.

-
- [1] B. Y. Dubetskii, A. P. Kazantsev, V. P. Chebotayev, and V. P. Yakovlev, Interference of atoms and formation of atomic spatial arrays in light fields, *Pis'ma Zh. Eksp. Teor. Fiz.* **39**, 531 (1984) [*JETP Lett.* **39**, 649 (1984)].
- [2] *Atom Interferometry*, edited by P. R. Berman (Academic, Cambridge, 1997).
- [3] *Atom Interferometry*, Proceedings of the International School of Physics "Enrico Fermi," Course CLXXXVIII, Varenna, 2013, edited by G. M. Tino and M. Kasevich (IOS, Amsterdam, 2014).
- [4] R. Geiger, A. Landragin, S. Merlet, F. P. D. Santos, High-accuracy inertial measurements with cold-atom sensors, *AVS Quantum Sci.* **2**, 024702 (2020).
- [5] Q. Zhang, Y. Wang, C. Zhu, Y. Wang, X. Zhang, K. Gao, and W. Zhang, Precision measurements with cold atoms and trapped ions, *Chin. Phys. B* **29**, 093203 (2020).
- [6] G. M. Tino, Testing gravity with cold atom interferometry: Results and prospects, in *Focus on Quantum Sensors for New-Physics Discoveries*, edited by M. Safronova and D. Budker, special issue of *Quantum Sci. Technol.* **6**, 024014 (2021).
- [7] A. Bertoldi, P. Bouyer, and B. Canuel, Quantum sensors with matter waves for GW observation, in *Handbook of Gravitational Wave Astronomy*, edited by C. Bambi, S. Katsanevas, and K. D. Kokkotas (Springer, Singapore, 2021).
- [8] C. Ufrecht, A. Roura, and W. P. Schleich, Bose-Einstein condensates in microgravity and fundamental tests of gravity, [arXiv:2107.03709](https://arxiv.org/abs/2107.03709).
- [9] A. Belenchia, M. Carlesso, Ö. Bayraktar, D. Dequal, I. Derkach, G. Gasbarri, W. Herr, Y. L. Li, M. Rademacher, J. Sidhu, D. K. L. Oi *et al.*, Quantum physics in space, *Phys. Rep.* **951**, 1 (2022).
- [10] I. Alonso, C. Alpigiani, B. Altschul, H. Araújo, G. Arduini, J. Arlt, L. Badurina, A. Balaž, S. Bandarupally, B. C. Barish *et al.*, Cold atoms in space: Community workshop summary and proposed road-map, *EPJ Quantum Technol.* **9**, 30 (2022).
- [11] S. Abend, B. Allard, A. S. Arnold, T. Ban, L. Barry, B. Battelier, A. Bawamia, Q. Beaufils, S. Bernon, A. Bertoldi *et al.*, Technology roadmap for cold-atoms based quantum inertial sensor in space, *AVS Quantum Sci.* **5**, 019201 (2023).
- [12] B. Canuel, S. Abend, P. Amaro-Seoane, F. Badaracco, Q. Beaufils, A. Bertoldi, K. Bongs, P. Bouyer, C. Braxmaier, W. Chaibi1 *et al.*, ELGAR—A European laboratory for gravitation and atom-interferometric research, *Class. Quantum Grav.* **37**, 225017 (2020).
- [13] M.-S. Zhan, J. Wang, W.-T. Ni, D.-F. Gao, G. Wang, L.-X. He, R.-B. Li, L. Zhou, X. Chen, J.-Q. Zhong *et al.*, ZAIGA: Zhaoshan long-baseline atom interferometer gravitation antenna, *Int. J. Mod. Phys. D* **29**, 1940005 (2020).
- [14] L. Badurina, E. Bentine, D. Blas, K. Bongs, D. Bortoletto, T. Bowcock, K. Bridges, W. Bowden, O. Buchmueller, C. Burrage *et al.*, AION: An atom interferometer observatory and network, *J. Cosmol. Astropart. Phys.* **2020**, 011 (2020)
- [15] B. Battelier, J. Bergé, A. Bertoldi, L. Blanchet, K. Bongs, P. Bouyer, C. Braxmaier, D. Calonico, P. Fayet, N. Gaaloul *et al.*, Exploring the foundations of the universe with space tests of the equivalence principle, *Exp. Astron.* **51**, 1695 (2021).
- [16] Y. A. El-Neaj, C. Alpigiani, S. Amairi-Pyka, H. Araújo, A. Balaž, A. Bassi, L. Bathe-Peters, B. Battelier, A. Belić, E. Bentine *et al.*, AEDGE: Atomic experiment for dark matter and gravity exploration in space, *EPJ Quantum Technol.* **7**, 6 (2020).
- [17] G. M. Tino, A. Bassi, G. Bianco, K. Bongs, P. Bouyer, L. Cacciapuoti, S. Capozziello, X. Chen, M. L. Chiofalo, A. Derevianko *et al.*, SAGE: A proposal for a space atomic gravity explorer, *Eur. Phys. J. D* **73**, 228 (2019).
- [18] M. Abe, P. Adamson, M. Borcean, D. Bortoletto, K. Bridges, S. P. Carman, S. Chattopadhyay, J. Coleman, N. M. Curfman, K. DeRose *et al.*, Matter-wave Atomic Gradiometer Interferometric Sensor (MAGIS-100), *Quantum Sci. Technol.* **6**, 044003 (2021).
- [19] R. Kaltenbaek, A. Acin, L. Bacsardi, P. Bianco, P. Bouyer, E. Diamanti, C. Marquardt, Y. Omar, V. Pruneri, E. Rasel *et al.*, Quantum technologies in space, *Exp. Astron.* **51**, 1677 (2021).
- [20] H. Ahlers, L. Badurina, A. Bassi, B. Battelier, Q. Beaufils, K. Bongs, P. Bouyer, C. Braxmaier, O. Buchmueller, M. Carlesso *et al.*, STE-QUEST: Space Time Explorer and Quantum Equivalence principle Space Test, [arXiv:2211.15412](https://arxiv.org/abs/2211.15412).
- [21] Q. Beaufils, J. Lefebvre, J. G. Baptista, R. Piccon, V. Cambier, L. A. Sidorenkov, C. Fallet, T. Lévêque, F. P. D. Santos, Rotation related systematic effects in a cold atom interferometer onboard a Nadir pointing satellite, *npj Micrograv.* **9**, 53 (2023).
- [22] S. M. Dickerson, J. M. Hogan, A. Sugarbaker, D. M. S. Johnson, and M. A. Kasevich, Multiaxis inertial sensing with long-time point source atom interferometry, *Phys. Rev. Lett.* **111**, 083001 (2013).
- [23] C. D. Panda, M. Tao, J. Egelhoff, M. Ceja, V. Xu, and H. Müller, Quantum metrology by one-minute interrogation of a coherent atomic spatial superposition, [arXiv:2210.07289](https://arxiv.org/abs/2210.07289).
- [24] T. Kovachy, S.-W. Chiow, and M. A. Kasevich, Adiabatic-rapid-passage multiphoton Bragg atom optics, *Phys. Rev. A* **86**, 011606(R) (2012).
- [25] J.-N. Kirsten-Siemß, F. Fitzek, C. Schubert, E. M. Rasel, N. Gaaloul, and K. Hammerer, Large-momentum-transfer atom interferometers with μrad -accuracy using Bragg diffraction, *Phys. Rev. Lett.* **131**, 033602 (2023).

- [26] P. Cladé, S. Guellati-Khélifa, F. Nez, and F. Biraben, Large momentum beam splitter using Bloch oscillations, *Phys. Rev. Lett.* **102**, 240402 (2009).
- [27] M. H. Goerz, M. A. Kasevich and V. S. Malinovsky, Robust optimized pulse schemes for atomic fountain interferometry, *Atoms* **11**, 36 (2023).
- [28] D. S. Weiss, B. C. Young, and S. Chu, Precision measurement of the photon recoil of an atom using atomic interferometry, *Phys. Rev. Lett.* **70**, 2706 (1993).
- [29] A. P. Kol'chenko, S. G. Rautian, and R. I. Sokolovskii, Interaction of an atom with a strong electromagnetic field with the recoil effect taken into consideration, *Zh. Eksp. Teor. Fiz.* **55**, 1864 (1968) [*JETP* **28**, 986 (1969)].
- [30] T. Kovachy, P. Asenbaum, C. Overstreet, C. A. Donnelly, S. M. Dickerson, A. Sugarbaker, J. M. Hogan, and M. A. Kasevich, Quantum superposition at the half-metre scale, *Nature (London)* **528**, 530 (2015).
- [31] B. Plotkin-Swing, D. Gochner, K. E. McAlpine, E. S. Cooper, A. O. Jamison, and S. Gupta, Three-path atom interferometry with large momentum separation, *Phys. Rev. Lett.* **121**, 133201 (2018).
- [32] T. Kovachy, J. M. Hogan, D. M. S. Johnson, and M. A. Kasevich, Optical lattices as waveguides and beam splitters for atom interferometry: An analytical treatment and proposal of applications, *Phys. Rev. A* **82**, 013638 (2010).
- [33] J. Rudolph, T. Wilkason, M. Nantel, H. Swan, C. M. Holland, Y. Jiang, B. E. Garber, S. P. Carman, and J. M. Hogan, Large momentum transfer clock atom interferometry on the 689 nm intercombination line of strontium, *Phys. Rev. Lett.* **124**, 083604 (2020).
- [34] M. Gebbe, J.-N. Siemß, M. Gersemann, H. Müntinga, S. Herrmann, C. Lämmerzahl, H. Ahlers, N. Gaaloul, C. Schubert, K. Hammerer, S. Abend, and E. M. Rasel, Twin-lattice atom interferometry, *Nat. Commun.* **12**, 2544 (2021).
- [35] R. H. Parker, C. Yu, W. Zhong, B. Estey, and H. Müller, Measurement of the fine-structure constant as a test of the standard model, *Science* **360**, 191 (2018).
- [36] E. Peik, M. B. Dahan, I. Bouchoule, Y. Castin, and C. Salomon, Bloch oscillations of atoms, adiabatic rapid passage, and monokinetic atomic beams, *Phys. Rev. A* **55**, 2989 (1997).
- [37] L. Morel, Z. Yao, P. Cladé, and S. Guellati-Khélifa, Determination of the fine-structure constant with an accuracy of 81 parts per trillion, *Nature (London)* **588**, 61 (2020).
- [38] M. A. Kasevich and B. Dubetsky, Kinematic sensors employing atom interferometer phases, US Patent 7,317,184 (8 January 2008).
- [39] B. Dubetsky, Local positioning system as a classic alternative to atomic navigation, *J. Navigation* **75**, 273 (2022).
- [40] M. Kasevich and S. Chu, Atomic interferometry using stimulated Raman transitions, *Phys. Rev. Lett.* **67**, 181 (1991).
- [41] F. Riehle, Th. Kisters, A. Witte, J. Helmcke, and Ch. J. Bordé, Optical Ramsey spectroscopy in a rotating frame: Sagnac effect in a matter-wave interferometer, *Phys. Rev. Lett.* **67**, 177 (1991).
- [42] E. M. Rasel, M. K. Oberthaler, H. Batelaan, J. Schmiedmayer, and A. Zeilinger, Atom wave interferometry with diffraction gratings of light, *Phys. Rev. Lett.* **75**, 2633 (1995).
- [43] S. B. Cahn, A. Kumarakrishnan, U. Shim, T. Sleator, P. R. Berman, and B. Dubetsky, Time-domain de Broglie wave interferometry, *Phys. Rev. Lett.* **79**, 784 (1997).
- [44] V. P. Chebotayev, B. Y. Dubetsky, A. P. Kazantsev, and V. P. Yakovlev, Interference of atoms in separated optical fields, *J. Opt. Soc. Am. B* **2**, 1791 (1985).
- [45] C. J. Bordé, Atomic interferometry with internal state labeling, *Phys. Lett. A* **140**, 10 (1989).
- [46] S. Hartmann, J. Jenewein, E. Giese, S. Abend, A. Roura, E. M. Rasel, and W. P. Schleich, Regimes of atomic diffraction: Raman versus Bragg diffraction in retroreflective geometries, *Phys. Rev. A* **101**, 053610 (2020).
- [47] B. Dubetsky and P. R. Berman, $\lambda/4$, $\lambda/8$ and higher order atom gratings via Raman transitions, *Laser Phys.* **12**, 1161 (2002).
- [48] T. Lévêque, A. Gauguier, F. Michaud, F. P. D. Santos, and A. Landragin, Enhancing the area of a Raman atom interferometer using a versatile double-diffraction technique, *Phys. Rev. Lett.* **103**, 080405 (2009).
- [49] E. Giese, A. Roura, G. Tackmann, E. M. Rasel, and W. P. Schleich, Double Bragg diffraction: A tool for atom optics, *Phys. Rev. A* **88**, 053608 (2013).
- [50] S. Hartmann, J. Jenewein, S. Abend, A. Roura, and E. Giese, Atomic Raman scattering: Third-order diffraction in a double geometry, *Phys. Rev. A* **102**, 063326 (2020).
- [51] M. Chiarotti, J. N. Tinsley, S. Bandarupally, S. Manzoor, M. Sacco, L. Salvi, and N. Poli, Practical limits for large-momentum-transfer clock atom interferometers, *PRX Quantum* **3**, 030348 (2022).
- [52] P. Asenbaum, C. Overstreet, M. Kim, J. Curti, and M. A. Kasevich, Atom-interferometric test of the equivalence principle at the 10^{-12} level, *Phys. Rev. Lett.* **125**, 191101 (2020).
- [53] S.-W. Chiow, T. Kovachy, H.-C. Chien, and M. A. Kasevich, $102\hbar k$ large area atom interferometers, *Phys. Rev. Lett.* **107**, 130403 (2011).
- [54] I. I. Rabi, Space quantization in a gyrating magnetic field, *Phys. Rev.* **51**, 652 (1937).
- [55] M. H. Levitt and R. Freeman, NMR population inversion using a composite pulse, *J. Magn. Reson.* **33**, 473 (1979).
- [56] J. Saywell, M. Carey, M. Belal, I. Kuprov, and T. Freegarde, Optimal control of Raman pulse sequences for atom interferometry, *J. Phys. B* **53**, 085006 (2020).
- [57] B. Dubetsky, Asymmetric Mach-Zehnder atom interferometers, [arXiv:1710.00020](https://arxiv.org/abs/1710.00020).
- [58] The expression (6b) at $n = 0$ was first derived for phases of the neutron interferometer; see Eq. (4.8) in the article by D. M. Greenberger and A. W. Overhauser, Coherence effects in neutron diffraction and gravity experiments, *Rev. Mod. Phys.* **51**, 43 (1979).
- [59] T. Sleator, P. R. Berman, and B. Dubetsky, High precision atom interferometry in a microgravity environment, [arXiv:physics/9905047](https://arxiv.org/abs/physics/9905047).
- [60] B. Dubetsky and P. R. Berman, Ground-state Ramsey fringes, *Phys. Rev. A* **56**, R1091 (1997).
- [61] B. Dubetsky and M. A. Kasevich, Atom interferometer as a selective sensor of rotation or gravity, *Phys. Rev. A* **74**, 023615 (2006).
- [62] K. Bongs, R. Launay, and M. A. Kasevich, High-order inertial phase shifts for time-domain atom interferometers, *Appl. Phys. B* **84**, 599 (2006).
- [63] B. Dubetsky, S. B. Libby, and P. Berman, Atom interferometry in the presence of an external test mass, *Atoms* **4**, 14 (2016).
- [64] P. Asenbaum, C. Overstreet, T. Kovachy, D. D. Brown, J. M. Hogan, and M. A. Kasevich, Phase shift in an atom

- interferometer due to spacetime curvature across its wave function, *Phys. Rev. Lett.* **118**, 183602 (2017).
- [65] B. Dubetsky and G. Raithel, Nanometer scale period sinusoidal atom gratings produced by a Stern-Gerlach beam splitter, [arXiv:physics/0206029](https://arxiv.org/abs/physics/0206029).
- [66] The inequality (25b) means that during the time Δ^{-1} one can neglect the changes in the phase of the wave function associated with the Raman frequency detuning $\tilde{\delta}$, with the Doppler shift (18b), and the change in this shift due to the acceleration of the atom $|\mathbf{q}_i \cdot \mathbf{g}|T$, with the recoil frequency (2), with characteristic times of change in the amplitude and phase of the fields τ_f and ϕ^{-1} . Under these conditions, one can eliminate the first term on the right-hand side of Eq. (24c) and then, using integration by parts, arrive at the expression (27) for the level $|o\rangle$ amplitude.
- [67] J. M. McGuirk, G. T. Foster, J. B. Fixler, M. J. Snadden, and M. A. Kasevich, Sensitive absolute-gravity gradiometry using atom interferometry, *Phys. Rev. A* **65**, 033608 (2002).
- [68] A. Louchet-Chauvet, T. Farah, Q. Bodart, A. Clairon, A. Landragin, S. Merlet, and F. P. D. Santos, The influence of transverse motion within an atomic gravimeter, *New J. Phys.* **13**, 065025 (2011).
- [69] Another possibility here is to place detunings Δ between sub-levels of the hyperfine structure of the state o so that the contributions to the ac Stark shift from different sublevels cancel each other.
- [70] L. D. Landau and E. M. Lifshitz, *Quantum Mechanics: Non-relativistic Theory* (Pergamon, Oxford, 1989), p. 205, problem 1.
- [71] A. Peters, High precision gravity measurements using atom interferometry, Ph.D. thesis, Stanford University, 1998.
- [72] C. Antoine, Matter wave beam splitters in gravito-inertial and trapping potentials: Generalized ttt scheme for atom interferometry, *Appl. Phys. B* **84**, 585 (2006).
- [73] A. Bertoldi, F. Minardi, and M. Prevedelli, Phase shift in atom interferometers: Corrections for nonquadratic potentials and finite-duration laser pulses, *Phys. Rev. A* **99**, 033619 (2019).
- [74] N. F. Ramsey, A new molecular beam resonance method, *Phys. Rev.* **76**, 996 (1949).
- [75] V. I. Yudin, A. V. Taichenachev, C. W. Oates, Z. W. Barber, N. D. Lemke, A. D. Ludlow, U. Sterr, C. Lisdat, and F. Riehle, Hyper-Ramsey spectroscopy of optical clock transitions, *Phys. Rev. A* **82**, 011804(R) (2010).
- [76] N. Huntemann, B. Lipphardt, M. Okhapkin, C. Tamm, E. Peik, A. V. Taichenachev, and V. I. Yudin, Generalized Ramsey excitation scheme with suppressed light shift, *Phys. Rev. Lett.* **109**, 213002 (2012).
- [77] A. C. Carew, Apparatus for inertial sensing with cold atoms, Ph.D. thesis, York University, 2018.
- [78] B. C. Young (private communication).
- [79] F. Di Pumpo, C. Ufrecht, A. Friedrich, E. Giese, W. P. Schleich, and W. G. Unruh, Gravitational redshift tests with atomic clocks and atom interferometers, *PRX Quantum* **2**, 040333 (2021).
- [80] B. Fang, N. Mielec, D. Savoie, M. Altorio, A. Landragin, and R. Geiger, Improving the phase response of an atom interferometer by means of temporal pulse shaping, *New J. Phys.* **20**, 023020 (2017).
- [81] J. F. Clauser, Ultra-high sensitivity accelerometers and gyroscopes using neutral atom matter-wave interferometry, *Physica B+C* **151**, 262 (1988).
- [82] I. Perrin, M. Cadoret, Y. Bidel, N. Zahzam, C. Blanchard, and A. Bresson, Proof-of-principle demonstration of vertical gravity gradient measurement using a single proof mass double-loop atom interferometer, *Phys. Rev. A* **99**, 013601 (2019).
- [83] J. K. Stockton, K. Takase, and M. A. Kasevich, Absolute geodetic rotation measurement using atom interferometry, *Phys. Rev. Lett.* **107**, 133001 (2011).
- [84] L. A. Sidorenkov, R. Gautier, M. Altorio, R. Geiger, and A. Landragin, Tailoring multi-loop atom interferometers with adjustable momentum transfer, *Phys. Rev. Lett.* **125**, 213201 (2020).
- [85] I. Dutta, D. Savoie, B. Fang, B. Venon, C. L. Garrido Alzar, R. Geiger, and A. Landragin, Continuous cold-atom inertial sensor with 1 nrad/sec rotation stability, *Phys. Rev. Lett.* **116**, 183003 (2016).
- [86] R. Gautier, M. Guessoum, L. A. Sidorenkov, Q. Bouton, A. Landragin, and R. Geiger, Accurate measurement of the Sagnac effect for matter waves, *Sci. Adv.* **8**, eabn8009 (2022).
- [87] A. P. Kazantsev and G. I. Surdutovich, The Kapitza-Dirac effect for atoms in a strong resonant field, *Pis'ma Zh. Eksp. Teor. Fiz.* **21**, 346 (1975) [*JETP Lett.* **21**, 158 (1975)].
- [88] A. Turlapov, A. Tonyushkin, and T. Sleator, Talbot-Lau effect for atomic de Broglie waves manipulated with light, *Phys. Rev. A* **71**, 043612 (2005).
- [89] T. Pfau, C. Kurtsiefer, C. S. Adams, M. Sigel, and J. Mlynek, Magneto-optical beam splitter for atoms, *Phys. Rev. Lett.* **71**, 3427 (1993).
- [90] R. Grimm, J. Söding, and Y. B. Ovchinnikov, Coherent beam splitter for atoms based on a bichromatic standing light wave, *Opt. Lett.* **19**, 658 (1994).
- [91] A. P. Kazantsev, G. I. Surdutovich, and V. P. Yakovlev, On the quantum theory of resonance scattering of atoms by light, *Pis'ma Zh. Eksp. Teor. Fiz.* **31**, 542 (1980) [*JETP Lett.* **31**, 509 (1980)].
- [92] P. L. Gould and D. E. Pritchard, Atoms interacting with standing light waves: Diffraction, diffusion and rectification, in *Coherent and Collective Interactions of Particles and Radiation Beams*, Proceedings of the International School of Physics "Enrico Fermi," Course CXXXI, Varenna, 1995, edited by A. Aspect, W. Barletta, and R. Bonifacio (IOS, Amsterdam, 1996), Vol. 131, p. 443.
- [93] B. Dubetsky and P. R. Berman, Atom gratings produced by large-angle atom beam splitters, *Phys. Rev. A* **64**, 063612 (2001).
- [94] W. Gerlach and O. Stern, Der experimentelle nachweis des magnetischen moments des silberatoms, *Z. Phys.* **8**, 110 (1922).
- [95] P. R. Berman, B. Dubetsky, and J. L. Cohen, High-resolution amplitude and phase gratings in atom optics, *Phys. Rev. A* **58**, 4801 (1998).
- [96] R. Gupta, J. J. McClelland, P. Marte, and R. J. Celotta, Raman-induced avoided crossings in adiabatic optical potentials: Observation of $\lambda/8$ spatial frequency in the distribution of atoms, *Phys. Rev. Lett.* **76**, 4689 (1996).
- [97] P. S. Jessen and I. H. Deutsch, Optical lattices, *Adv. At. Mol. Opt. Phys.* **37**, 95 (1996).
- [98] B. Dubetsky and P. R. Berman, $\lambda/8$ -period optical potentials, *Phys. Rev. A* **66**, 045402 (2002).